

Institut für Wissenschaftliches Rechnen

Prof. Hermann G. Matthies, Ph.D.



der TU Braunschweig

Jahresbericht 2014

**Institut für Wissenschaftliches Rechnen
der TU Braunschweig**

Institutsvorstand: Prof. Hermann G. Matthies, Ph.D.
Geschäftszimmer: Frau Cosima Meyer, M.A.

Anschrift: Institut für Wissenschaftliches Rechnen
TU Braunschweig
Hans-Sommer-Str. 65
38106 Braunschweig

Telefon, Telefax: 0531/391-3000, 0531/391-3003
E-Mail: wire@tu-bs.de
URL: <http://www.wire.tu-bs.de>

Wissenschaftliche Mitarbeiterinnen, Mitarbeiter und Doktoranden:

Frau Dr.-Ing. Noémi Friedman
Herr Dr. rer. nat. Thorsten Grahs
Herr Dr. rer. nat. Martin Krosche
Herr Dr.-Ing. Rainer Niekamp
Herr Dr. rer. nat. Joachim Rang
Frau Dr.-Ing. Bojana Rosić
Herr Muhammad Sadiq Sarfaraz
Herr Dr. rer. nat. Elmar Zander

Stipendiaten im Deutsch-Italienischen Promotionsprogramm

Frau Ing. Valentina Chiarello
Herr Ing. Alberto Ciavattone
Frau Ing. Irene Simonetti
Herr Ing. Emanuele El Basri
Herr Ing. Giovanni Stabile

Assoziiert an der Tschechischen Technischen Universität Prag:

Frau Dr.-Ing. Anna Kučerová
Herr Dr.-Ing. Jan Sýkorá

Centre for Scientific Computing:

Herr Dr. rer. nat. Thorsten Grahs

Apl. Professor: Herr Dr.-Ing. habil. Joachim Axmann
(Volkswagen AG)

Inhaltsverzeichnis

1	Vorwort	6
2	Forschung	7
2.1	Stability analysis of a highlift public aircraft through uncertainty quantification of its eigenmotions	7
2.2	Uncertainty quantification for the numerical simulation of powder compactification processes	12
2.3	Centre of Scientific Computing	13
2.4	The Prothero and Robinson example: Convergence studies for Runge–Kutta and Rosenbrock–Wanner methods	15
2.5	An analysis of the Prothero–Robinson example for constructing new adaptive ESDIRK methods	18
2.6	A component framework for the parallel solution of the incompressible Navier-Stokes equations	21
2.7	Prediction of damage in bridge structures	25
2.8	Stochastic non-local models of irreversible behavior	29
2.9	Adaptive schemes for stochastic PDEs	33
2.10	Hydrological extreme events analysis for flood risk mitigation	37
2.11	A fault detection algorithm for an alternate aerobic/anoxic cycle nitrogen removal process.	41
2.12	Numerical Modelling and Optimization of Oscillating Water Column Wave Energy Converters	47
2.13	A numerical approach to the dynamics analysis of marine cables	53
3	Lehre im WS 2013/2014 and SS 2014	62
3.1	Wintersemester 2013/2014	62
3.2	Sommersemester 2014	62
4	Veröffentlichungen und Vorträge	63
4.1	Schriften und Proceedings	63
4.2	Berichte	66
4.3	Vorträge	67
4.4	Projekttreffen	69
4.5	Organisation von Minisymposia/Konferenzen	70

4.6	Teilnahme und Lehre an Workshops und Weiterbildung	71
4.7	Habilitation und Dissertationen	71
4.8	Abschluss- und Studienarbeiten	71
5	Sonstiges	71
5.1	Gäste am Institut	71
5.2	Einladungen an Mitglieder des Instituts	72
5.3	Board Memberships	72
5.4	Beteiligung am IRTG 1627	72
5.5	Beteiligung am Projekt „Isogeometric and stochastic collocation methods for nonlinear, probabilistic multi-scale problems in continuum mechanics“ im SPP 1748	73
5.6	Beteiligung am SFB 880 Fundamentals of High Lift for Future Civil Aircraft	74
5.7	Beteiligung am Studiengang CSE	74

1 Vorwort

Dear Reader,

in the last year one dissertation by Alberto Ciavattore (s. 4.7) was completed in the framework of the cooperation of TU Braunschweig with the University of Florence. The collaborative research centre SFB 880 was granted an extension by the DFG. We continue our work there, which will be further uncertainty quantification of high-lift aircraft configurations, as well as parameter identification of turbulence models for flow over porous media. Two new DFB collaborative efforts have been started, one is the international research training group IRTG 1627 on virtual materials in cooperation with the LU Hannover and ENS Cachan (Paris), and the other one is the DFB priority programme SPP 1748 on reliable simulation techniques in solid mechanics, where our work (jointly with Prof. Laura de Lorenzis) deals with isogeometric and stochastic collocation methods. As was evident last year, again in many cooperations our research deals with risk, stochastic computations, identification, or some such combinations. In particular the topic of identification by stochastic Bayesian methods has become computationally feasible through new applications of low-rank tensor approximation techniques.

I hope the reader will enjoy to see this interplay of subjects and the uses to which such methods can be put in the following pages.

Sincerely Yours

Hermann G. Matthies

2 Forschung

2.1 Stability analysis of a highlift public aircraft through uncertainty quantification of its eigenmotions

Ansprechpartner: Noémi Friedman, Elmar Zander,
 Joachim Rang, ¹Jobst H. Diekmann
 EMail: n.friedman@tu-bs.de
 Telefon: 0531/391-3013

¹ Institute of Flight Systems, DLR, Braunschweig

2.1.1 Introduction

Within the framework of the SFB 880 a new medium range civil aircraft with an active high lift system based on an internally blown flap system, that can take off and land on relatively short runways, was proposed [8]. The new aircraft design is intended to promote mobility in Europe through increasing the capacity of existing airports by an extended usage of the small airports in the close vicinity of bigger cities. This contribution focuses on the maneuverability and stability of the proposed aircraft which was analysed by extending its deterministic dynamic simulation model to the stochastic dimension. By this extension the aircraft behaviour is analysed in a probabilistic setting which can already include the uncertainties of the aerodynamical parameters of the model, like lift coefficients, drag coefficients, etc. It was earlier shown in [5] how this extension can be done in a non-intrusive manner, meaning without significantly changing the deterministic solver. There, the method was presented and tested through the analysis of a preliminary simulation model of a similar, turbo propeller engine driven aircraft. Here, we focus on the proposed active high lift configuration model. To analyse the controllability of the aircraft, the propagation of uncertainties and sensitivities of the response when perturbing the aircraft in the full-flap configuration before landing were investigated. Herein, a surrogate model is used applying the general Polynomial Chaos Expansion [9](furthermore gPCE). The coefficients of the expansion are calculated with two methods, collocation [1] and direct projection [2].

2.1.2 The deterministic simulation model

The non-linear deterministic simulation model describes the dynamic behaviour of the active high lift aircraft [3], and is governed by the equations of motion. For the maneuverability analysis, the aircraft eigenmotions were triggered by a sudden perturbation of the pitch rate in

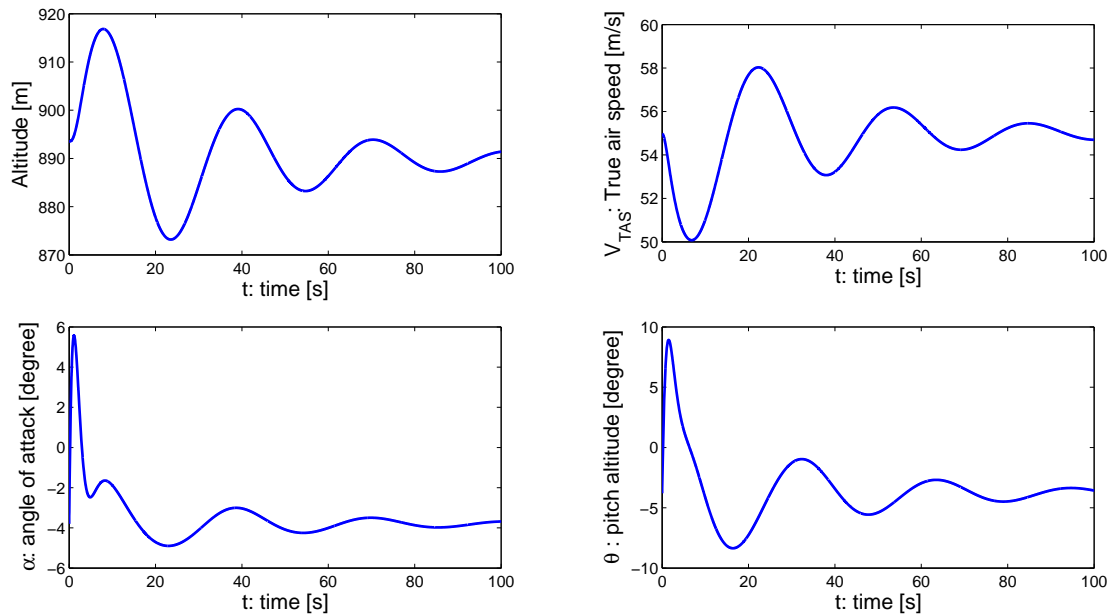


Figure 1: Triggering the eigenmotion: the deterministic response of the aircraft after perturbing the pitch rate of the trimmed aircraft (calculated with the expected values of the aerodynamic parameters)

unaccelerated horizontal flight and in the full flap configuration of the aircraft, at altitude 893.5 m, and with 55m/s true air speed. The perturbation triggers two damped oscillatory eigenmotions, called the short period and the phugoid motions. Figure 1 shows the response of the aircraft to this perturbation.

2.1.3 Numerical results

Uncertainty of the responses is due to variations of the aerodynamic parameters of the simulation model. Table 1 shows the mean values as well as the uncertainties of these parameters determined by professional experience. In the analysis, the 16 parameters with uncertainties were assumed to be independent random variables. For the probability distribution uniform probabilities were assigned within the given boundaries. The response surface was approximated by general Polynomial Chaos Expansion (furthermore gPCE) [9] using the multivariate Legendre polynomials of maximal order two, which was shown to be sufficient for the aim of the analysis. The coefficients of the gPCE were determined through collocation and direct projection methods using Smolyak sparse grid [6, 4, 10] for the numerical integration. The two methods gave similar results. Propagation of sensitivities were quantified by evaluating the first Sobolev indices [7] from the gPCE coefficients. The propagation of uncertainties (mean values and the 3σ region and coefficient of variation) of four responses and their sensitivities to the different uncertain parameters are shown in Fig. 2.

	C_μ	C_{L0}			$C_{L\alpha}$		
		C_{L0-cl+}	ΔC_{L-FL+}	ΔC_{L-DN}	$C_{L\alpha-cl+}$	$C_{L\alpha-FL+}$	$C_{L\alpha-DN}$
μ	0.0330	0.34454	2.8077	-0.4444	4.7344	-1.2368	0.3103
dev.	$\pm 5\%$	± 0.15	-	-	$\pm 5\%$	$\pm 5\%$	$\pm 5\%$
		C_{D0}					
		C_{D0-cl+}	$\Delta C_{D0-HTP+}$	ΔC_{D0-FL+}	ΔC_{D0-DN}		
μ		0.0209	0.0043	0.0506	0.2263		
dev.		± 0.05	-	-	-		
		k_1			k_2		
		k_{1-cl+}	Δk_{1-FL+}	Δk_{1-DN}	k_{2-cl+}	Δk_{2-FL+}	Δk_{2-DN}
μ		0.0105	-0.0105	-0.1316	0.0351	0.0062	0.0200
dev.		$\pm 10\%$	$\pm 10\%$	$\pm 10\%$	$\pm 10\%$	$\pm 10\%$	$\pm 10\%$
		C_{m0}			$C_{m\alpha}$		
		C_{m0+}	$C_{m0-HTP+}$	ΔC_{m0-FL}	$C_{m\alpha-cl+}$	$\Delta C_{m\alpha-FL+}$	$\Delta C_{m\alpha-DN}$
μ		-0.1194	-0.5845	0.0268	0.9863	-0.3392	0.2708
dev.		± 0.15	-	-	$\pm 5\%$	$\pm 5\%$	$\pm 5\%$

Table 1: Description of the random parameters, and their components: C_μ - jet momentum coefficient, C_{L0} - lift coefficient at zero angle of attack, $C_{L\alpha}$ - lift coefficient curve slope, C_{D0} - drag coefficient at zero angle of attack, k_1 , k_2 - linear and quadratic coefficients for the induced drag, C_{m0} - pitching moment at zero angle of attack, $C_{m\alpha}$ - pitching moment curve slope. Indices of components: *cl* - value for clean cruise configuration, *FL* - shift of value due to full-flap configuration, *DN* - shift of value due to droop nose, *HTP* - shift of value due to the horizontal tail plane

2.1.4 Conclusion, outlook

The herein drafted investigations showed no concerns regarding the longitudinal stability of the new aircraft design, however, the given uncertainties of the dynamical parameters results in very high coefficients of variation, which for some responses may exceed 20%. The sensitivity analysis showed some trivial and non-trivial dependencies of the response of the aircraft. For example sensitivities to variations of the jet-momentum coefficient provided new information.

For further evaluation of the new aircraft design, the uncertainties are planned to be quantified also in the frequency domain. The boundaries of the eigenfrequencies and the damping ratios are classical indicators for the classification of the aircraft stability. In engineering practice, this is usually done with a Monte Carlo simulation. The herein used surrogate model using sparse grid integration rule can highly speed up the conventional evaluation method.

References

- [1] I. Babuška, F. Nobile, and R. Tempone, *A stochastic collocation method for elliptic partial differential equations with random input data*, SIAM Review **52** (2010), no. 2, 317–355, [doi:10.1137/100786356](https://doi.org/10.1137/100786356).

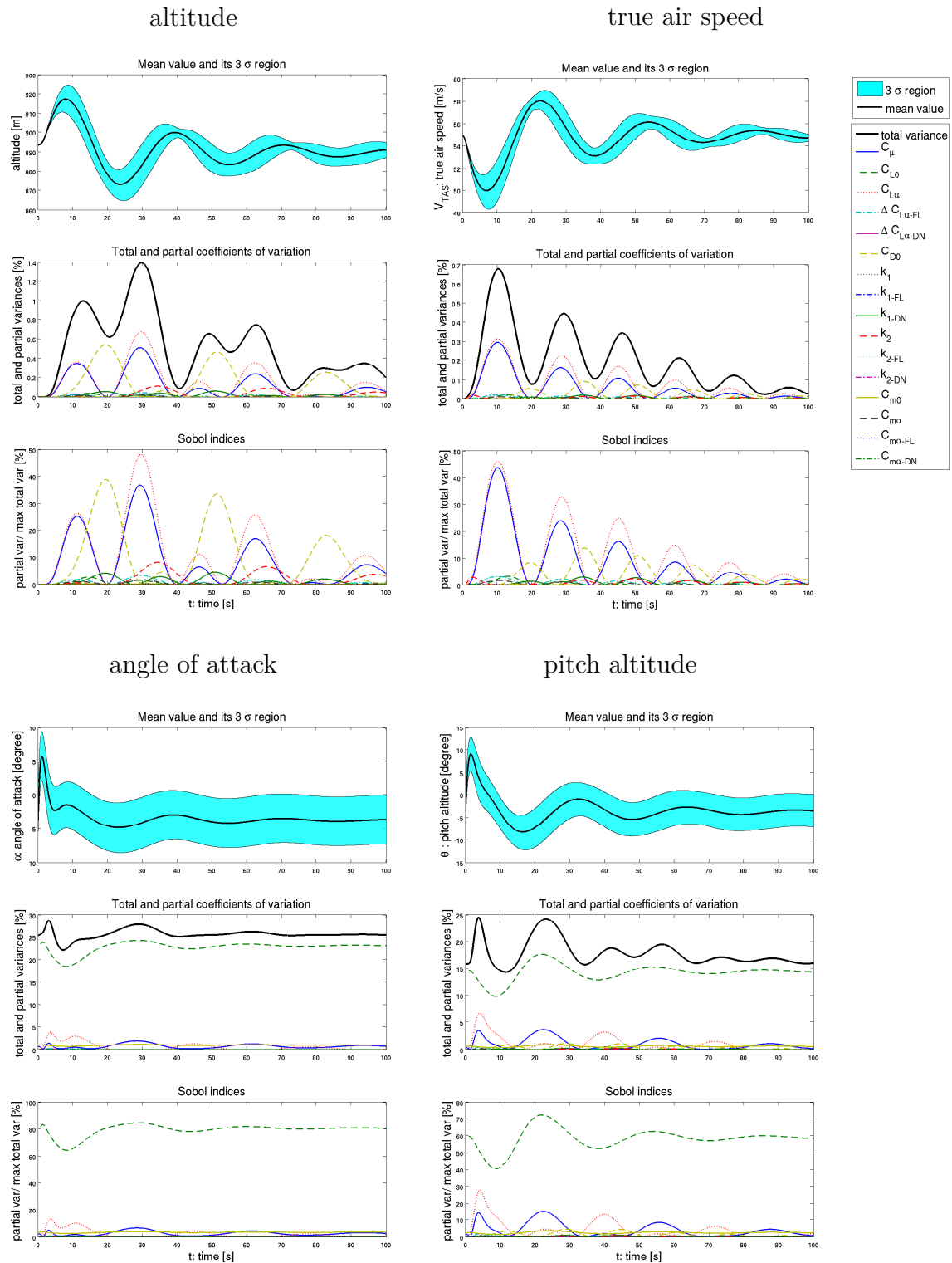


Figure 2: Propagation of uncertainties (mean value and the 3σ region), propagation of coefficient of variation (variance/maximum of the mean value) and propagation of sensitivities (first Sobol' indices) of four responses of the aircraft to perturbation

-
- [2] P. G. Constantine, M. S. Eldred, and E. T. Phipps, *Sparse pseudospectral approximation method*, Computer Methods in Applied Mechanics and Engineering **229-232** (2012), 1–12, [doi:10.1016/j.cma.2012.03.019](https://doi.org/10.1016/j.cma.2012.03.019).
- [3] J. H. Diekmann and K.-U. Hahn, *Nonlinear flight dynamics simulation model for a civil aircraft with active high lift system*, SFB 880 - Fundamentals of high-lift for future commercial aircraft (R. Radespiel and R. Semaan, eds.), TU Braunschweig - Campus Forschungsflughafen, 2013.
- [4] E. Novak and K. Ritter, *High dimensional integration of smooth functions over cubes*, Numerische Mathematik **75** (1996), 79–97, [doi:10.1016/j.res.2007.04.002](https://doi.org/10.1016/j.res.2007.04.002).
- [5] B. Rosić and A. Diekmann, J. *Methods for the uncertainty quantification of aircraft simulation models*, AIAA, Journal of Aircraft (2014), [doi:10.2514/1.C032856](https://doi.org/10.2514/1.C032856).
- [6] A. Smolyak, S. *Quadrature and interpolation formulas for tensor products of certain classes of functions*, Soviet Mathematics Doklady **4** (1963), 240–243.
- [7] B. Sudret, *Global sensitivity analysis using polynomial chaos expansions*, Reliability Engineering and System Safety **93** (2008), no. 7, 964–979, [doi:10.1016/j.res.2007.04.002](https://doi.org/10.1016/j.res.2007.04.002).
- [8] T. Weiss and W. Heinze, *Multidisciplinary design of cestol aircraft with powered lift system*, SFB 880 - Fundamentals of high-lift for future commercial aircraft (R. Radespiel and R. Semaan, eds.), TU Braunschweig - Campus Forschungsflughafen, 2013.
- [9] D. Xiu and G. Karniadakis, *The Wiener–Askey polynomial chaos for stochastic differential equations*, SIAM Journal on Scientific Computing **24** (2002), no. 2, 619–644, [doi:10.1137/S1064827501387826](https://doi.org/10.1137/S1064827501387826).
- [10] D. Xiu and J. S. Hesthaven, *High-order collocation methods for differential equations with random inputs*, SIAM Journal on Scientific Computing **27** (2005), no. 3, 1118–1139, [doi:10.1137/040615201](https://doi.org/10.1137/040615201).

2.2 Uncertainty quantification for the numerical simulation of powder compactification processes

Ansprechpartner:	Thorsten Grahs
E-Mail:	t.grahs@tu-bs.de
Telefon:	0531/391-3008

The investigation on uncertainty quantification in powder compactification simulations is carried out within a common research project of the Niedersächsische Technische Hochschule (NTH). Collaboration partners are the Institute of Mechanics, Technische Universität Clausthal (TUC) and the Institute of Continuum Mechanics, Leibniz Universität Hannover (LUH), respectively.

Within this project the simulation process of powder compactification process should be improved. The goal of the project is to gain a more detailed understanding of the deformation process inside the form, particularly with regard to the arising uncertainties within the simulation process. Here, a robust method for quantification of the uncertainties should be developed. Examples for areas where these uncertain parameter arise from are f.i. the material model, boundary and contact conditions.

As simulation tool, the Finite Element program TASAFEM, developed at the Institute of Mechanics, TUC, is considered. Here, a three-dimensional formulation of the powder compactification process is given (see [1, 2, 4]).

In a first step, a reduced simulation model with a Neo-Hookian material model is coupled to several uncertainty quantification algorithms and several detailed simulation are carried out. Used algorithms for the UQ process were the Monte Carlo (MC) method, Quasi Monte Carlo (QMC) method and a stochastic collocation approach.

In the next step, a non-intrusive Galerkin approach ([3]) should be applied to these test cases and extended later to visco-plastic materials.

Beside this, a discrete element method (DEM), ([5, 6, 7]) designed by the Institut of Mechanics, LUH is involved in the project in order to use homogenisation techniques for coupling of solid bodies and particle simulation. The DEM method will be used, in order to derive advanced material models for the numerical simulation of the powder compactification process. Here, Uncertainty quantification is used to improve the force model which is used inside the DEM simulation.

References

- [1] W. Bier, *Constitutive model for metal powder and its numerical treatment using finite elements*, Phd-thesis published as report no. 1/2008, Institute of Mechanics, University of Kassel, 2008.
- [2] W. Bier and S. Hartmann, *A finite strain constitutive model for metal powder compactation using a unique and convex single surface yield function*, European Journal of Mechanics, Series A/Solids **25** (2006), 1009 – 1030.
- [3] L. Giralardi, A. Litvinenko, D. Liu, H. G. Matthies, and A. Nouy, *To Be or Not to Be Intrusive? the solution of parametric and stochastic equations – the Plain Vanilla Galerkin Case*, SIAM J. Sci. Comput. **36** (2014), no. 6, 2729 – 2744.
- [4] S. Hartmann and W. Bier, *High-order time integration applied to metal powder plasticity*, International Journal of Plasticity **24** (2008), no. 1, 17 – 54.
- [5] C. Wellmann, *A two-scale method of granular materials using a coupled de-fe approach*, Phd-thesis, Institute of Continuum Mechanics, Leibniz University of Hannover, 2011.
- [6] C. Wellmann and P. Wriggers, *Homogenization of granular material modeled by a 3d dem*, Particle-Based Methods. Fundamentals and Applications (E. Oñate and D. R. J. Owen, eds.), Springer Verlag, Berlin, 2011.
- [7] C. Wellmann and P. Wriggers, *A two-scale model of granular materials*, Comp. Methods Appl. Mech. Engrg. **205** (2012).

2.3 Centre of Scientific Computing

Ansprechpartner: Thorsten Grahs EMail: t.grahs@tu-bs.de Telefon: 0531/391-3008
--

The Centre of Scientific Computing (CSC) is a joint research centre of the Institutes of Scientific Computing (Prof. Matthies) and Computational Mathematics (Prof. Sonar) within the Innovationsgesellschaft TU Braunschweig (iTUBS). The purpose of the centre is consulting and project management for problems from applied mathematics and scientific computing

2.3.1 Work carried out

In 2014 several research and training courses concerning the simulation tool-box OpenFOAM have been conducted. Also the 2nd Northern Germany OpenFoam user meeting was organized (see below).

Further more, talks and articles are published ([1, 2, 3])

Training courses

- OpenFOAM introduction
March, September and December 2014, TU Braunschweig
- OpenFOAM advanced
March and September 2014, TU Braunschweig
- OpenFOAM programming
September 2014, TU Braunschweig
- OpenFOAM Thermo simulation
December 2014, TU Braunschweig

Workshop organisation

- **2nd Northern germany OpenFoam User MeetiNg**
NOFUN 2014 – Braunschweig, Haus d. Wissenschaften, 24.09.2014.
With participants from DLR, FH Kiel, TU Berlin, Univ. Rostock, LU Hannover, TU Braunschweig, BETA systems, CPU 24|7, Engys, ...

References

- [1] T. Grahs and C. F. Janßen, *GPU-beschleunigte Mehrphasensimulationen für komplexe maritime Anwendungen*, Proc. NAFEMS Konferenz, Berechnung und Simulation: Anwendung, Entwicklung, Trends, Bamberg, 2014.
- [2] C. F. Janßen and T. Grahs, *Hochleistungsrechnen auf Grafikkarten für innovative Anwendungen in der Automobilindustrie*, NAFEMS Magazin **32** (2014), no. 4, 86 – 96.
- [3] C. F. Janßen and T. Grahs, *Realitätsprüfung – GPU-computing in der Automobilentwicklung*, Digital Engineering **8** (2014), 18 – 20.

2.4 The Prothero and Robinson example: Convergence studies for Runge–Kutta and Rosenbrock–Wanner methods

Ansprechpartner: Joachim Rang
 EMail: j.rang@tu-bs.de
 Telefon: 0531/391-3007

In the simulation of stiff ODEs and differential algebraic equations (DAEs), Runge–Kutta (RK) and Rosenbrock–Wanner (ROW) methods seem to be a good choice since these classes of methods include A -stable schemes. A -stability guarantees in general a stable numerical solution. One disadvantage of one-step methods is the order reduction phenomenon for stiff problems such as the example of Prothero and Robinson given by

$$\dot{u} = \lambda(u - \varphi(t)) + \dot{\varphi}(t), \quad u(0) = \varphi(0)$$

For Runge–Kutta methods Frank, Schneid and Ueberhuber in [1] introduced the concept of B -consistency and B -convergence. They show that B -consistency and B -stability imply B -convergence. In contrast to implicit Runge–Kutta methods Rosenbrock–Wanner methods can not be B -stable (see [2]). Scholz introduces B -consistency for Rosenbrock–Wanner methods [5] and proves that strongly A -stable Rosenbrock–Wanner methods are B -convergent if they are B -consistent. Moreover, order conditions are presented such that B -consistent Rosenbrock–Wanner methods can be developed.

In this project we introduce the concept of B_{PR} -consistency and B_{PR} -convergence similar to the concept of B -consistency and B -convergence. We can show that a B_{PR} -consistent one-step method of order q , which is A -stable with $R(\infty) < 1$, is B_{PR} -convergent of order q .

One aim of this project is the derivation of the local error. Therefore we apply Runge–Kutta method with a regular coefficient matrix A on the Prothero–Robinson example. From the representation of the local error we get new order conditions (see [4])

$$\mathbf{b}^\top \mathbf{A}^{-1} \mathbf{c}^k = 1, \quad k = 2, \dots, \bar{q}, \quad (1)$$

$$\mathbf{b}^\top \mathbf{A}^{-(l+1)} \frac{1}{k-l} \mathbf{c}^{k-l} = \mathbf{b}^\top \mathbf{A}^{-l} \mathbf{c}^{k-l-1}, \quad (2)$$

for $l = \max\{1, k - \bar{q}\}, \dots, k - 1$ and $k = 1, \dots, \infty$. A Runge–Kutta method is B_{PR} -consistent of order \bar{q} if condition (1) is satisfied for $k = 2, \dots, \bar{q}$ and (2) for $k = 2, \dots, \infty$ and $l = \max\{1, k - \bar{q}\}, \dots, k - 2$.

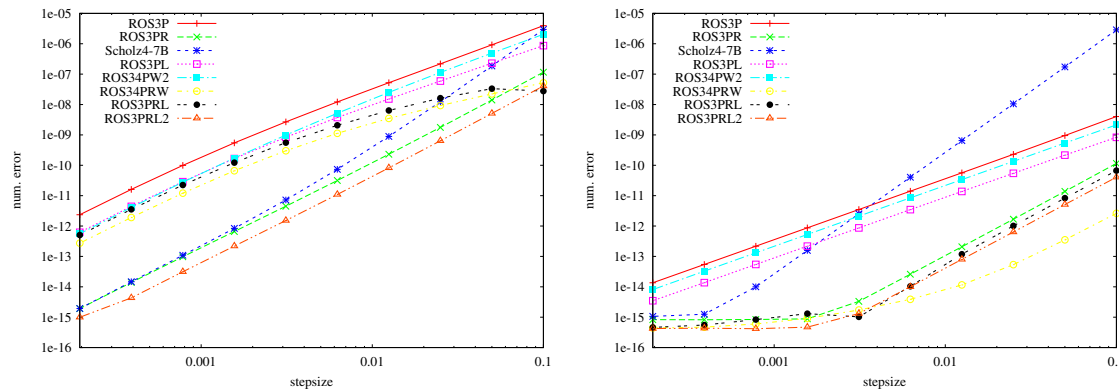
In [4] a B_{PR} -consistent method of order 2 with 4 internal stages is created. The coefficients of this method SDIRK2PR2 are presented in Table 2. This method converges with order 2 for all values $\lambda < 0$ in the

Table 2: Set of coefficients for the SDIRK2PR2 method

a_{21}	$= 2.071067811865475e - 01$	a_{22}	$= 2.928932188134525e - 01$
a_{31}	$= 7.071067811865476e - 01$	a_{32}	$= 0.000000000000000e + 00$
a_{33}	$= 2.928932188134525e - 01$	a_{41}	$= 1.121320343559643e + 00$
a_{42}	$= -5.857864376269050e - 01$	a_{43}	$= 1.715728752538099e - 01$
a_{44}	$= 2.928932188134525e - 01$		
b_1	$= 1.121320343559643e + 00$	\hat{b}_1	$= 7.071067811865476e - 01$
b_2	$= -5.857864376269050e - 01$	\hat{b}_2	$= 0.000000000000000e + 00$
b_3	$= 1.715728752538099e - 01$	\hat{b}_3	$= 2.928932188134525e - 01$
b_4	$= 2.928932188134525e - 01$	\hat{b}_4	$= 0.000000000000000e + 00$

case of the example of Prothero and Robinson although the stage order is only one.

A similar analysis can be made for Rosenbrock–Wanner methods which lead to similar order conditions as above. B_{PR} -consistent ROW methods of order 3 can be found in In [3] and [4]. Next we compare the theoretical results with the the numerical ones and consider the Prothero–Robinson example with $\varphi(t) = 10 - (10 + t) \exp(-t)$. We solve

Figure 3: τ versus error with $\lambda = -10^3$ (left) and $\lambda = -10^6$ (right)

this problem in the time interval $(0, 2]$ and take the discrete l_2 -error. As step-sizes we use $\tau = 0.1 \cdot 2^{-l}$, where $l = 0, \dots, 10$.

In the left part of Figure 3 we consider the medium stiff case, i.e. $\lambda = -10^3$ and in the right part the stiff case with $\lambda = -10^6$. In both cases it can be observed that B_{PR} -consistent methods such as ROS3PRL2 give much better results than non- B_{PR} -consistent methods such as ROS3PL. If a method is non- B_{PR} -consistent but satisfies only some conditions of equation (2) good results are computed in the stiff case but not in the medium case (see for example the ROS3PRL method). This effect can be observed in Figure 4, too, where we plot the stiffness factor $|\lambda|$ against the numerical order of convergence. For $|\lambda| = 10^3$ the numerical order of convergence drops down to one. B_{PR} -consistent methods such as ROS3PRL2 converge with order 3 for all values of λ .

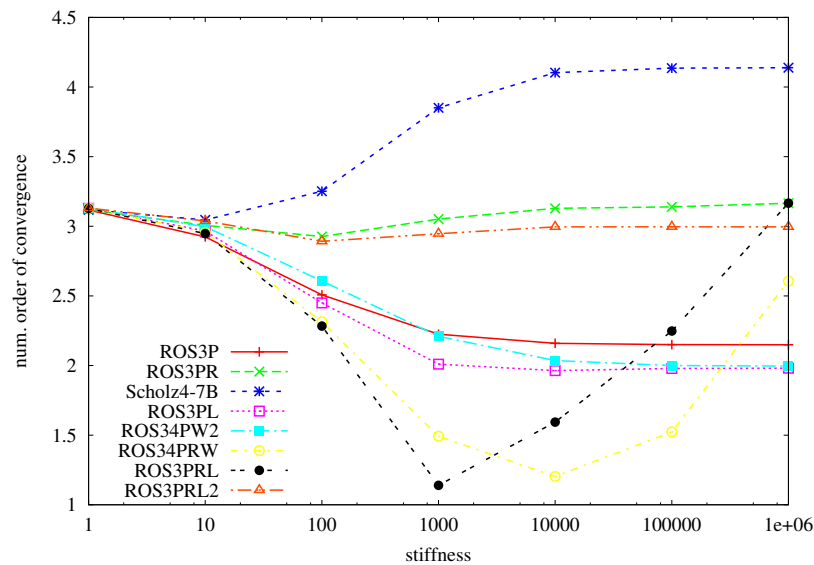


Figure 4: λ versus numerical order of convergence

References

- [1] R. Frank, J. Schneid, and C. W. Ueberhuber, *The concept of B-convergence*, SIAM J. Numer. Anal. **18** (1981), no. 5, 753–780.
- [2] E. Hairer and G. Wanner, *Solving ordinary differential equations. II: Stiff and differential-algebraic problems*, Springer Series in Computational Mathematics, vol. 14, Springer-Verlag, Berlin, 1996.
- [3] J. Rang, *Improved traditional Rosenbrock–Wanner methods for stiff ODEs and DAEs*, Informatik-Bericht 2013-05, TU Braunschweig, Braunschweig, 2013, URL: <http://www.digibib.tu-bs.de/?docid=00055262>.
- [4] J. Rang, *The Prothero and Robinson example: Convergence studies for Runge–Kutta and Rosenbrock–Wanner methods*, Informatik-Bericht 2014-08, TU Braunschweig, Braunschweig, 2014, URL: <http://www.digibib.tu-bs.de/?docid=00057194>.
- [5] S. Scholz, *Order barriers for the B-convergence of ROW methods*, Computing **41** (1989), no. 3, 219–235 (English), doi:10.1007/BF02259094.

2.5 An analysis of the Prothero–Robinson example for constructing new adaptive ESDIRK methods

Ansprechpartner: Joachim Rang
 EMail: j.rang@tu-bs.de
 Telefon: 0531/391-3007

In this project we apply the theory from chapter 2.4 to diagonally implicit Runge–Kutta (DIRK) methods with an explicit first stage (ESDIRK methods). These methods are widely used in the solution of ODEs and PDEs [3, 2], but the order reduction phenomenon can be observed. The order reduction can be decreased if order conditions for index-2 DAEs are satisfied. But when these methods are applied on medium stiff problems strong order reduction may be observed, although the numerical approximations are of good quality [7].

Next we apply ESDIRK methods on the example of Prothero–Robinson. The analysis of the local error leads to the following order conditions:

$$b_1 + \tilde{\mathbf{b}}^\top \tilde{A}^{-1}(\tilde{\mathbf{c}} - \mathbf{a}_1) = 1 \quad (3)$$

$$\tilde{\mathbf{b}}^\top \tilde{A}^{-1} \tilde{\mathbf{c}}^k = 1, \quad k = 2, \dots, p, \quad (4)$$

$$\tilde{\mathbf{b}}^\top \left[\tilde{A}^{-k}(\tilde{\mathbf{c}} - \mathbf{a}_1) - \tilde{A}^{-k+1} \tilde{\mathbf{e}} \right] = 0, \quad k = 2, \dots, p, \quad (5)$$

$$\tilde{\mathbf{b}}^\top \tilde{A}^{-l} \left[\tilde{A}^{-1} \tilde{\mathbf{c}}^{k-l} - (k-l) \tilde{\mathbf{c}}^{k-l-1} \right] = 0, \quad (6)$$

for $k = 2, \dots, \infty$ and $l = \max\{1, k-p\}, \dots, k-2$. In [6] new methods are created but these methods are not B_{PR} -consistent of order 3, i.e. they have order reduction if they are applied on medium stiff problems. The reason for this behaviour can be explained with the help of the remainder, which is given by terms of the form τ^k/z^l , where $z := \lambda\tau$.

As a numerical result we consider the differential-algebraic equation (see [4])

$$\begin{cases} \dot{u}_1 - u_3 \dot{u}_2 + u_2 \dot{u}_3 = 0 \\ u_2 = \epsilon \sin(\omega t) \\ u_3 = \epsilon \cos(\omega t) \\ u_1(0) = 0 \end{cases}, \quad (7)$$

which has differentiation index 1, but perturbation index 2 ([1, page 461]). Numerical results applied on this problem should be designed in such a way that order conditions for index-2 DAEs are satisfied (see [5]). For our numerical experiments we chose $\epsilon = 1$ and $\omega = 25$. First we solve this problem in the time interval $(0, 1/10]$ with equidistant time steps $\tau = 2.0 \cdot (1/2)^k$, where $k = 0, \dots, 5$. We present the numerical results in Figure 5. Methods such as ESDIRK32a, -43a and so on, which are not designed for index-2 DAEs, give the most inaccurate results. For the

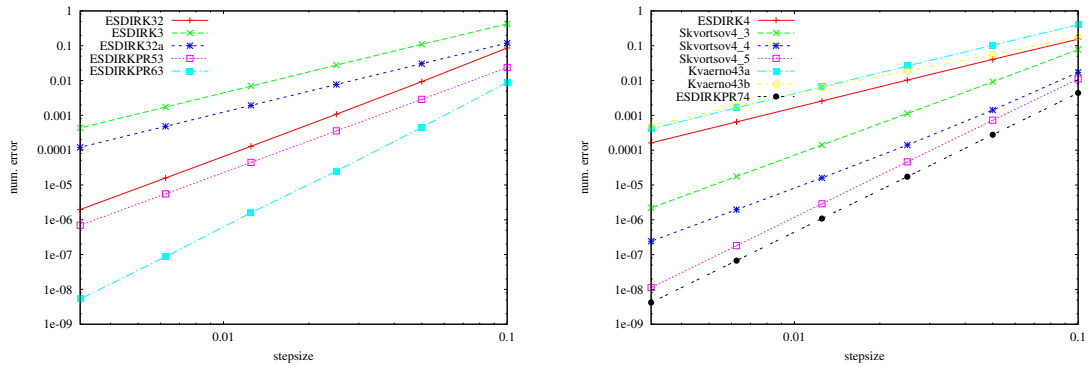


Figure 5: The solution of the index-2 DAE with constant step sizes: third order methods (left) and fourth order methods (right)

third order methods our new methods ESDIRK53PR and ESDIRK63PR are better than the ESDIRK32 method. In the case of the fourth order methods our new scheme ESDIRK74PR gives similar results as the Skvortsov4-5 method, but this method has no embedded method.

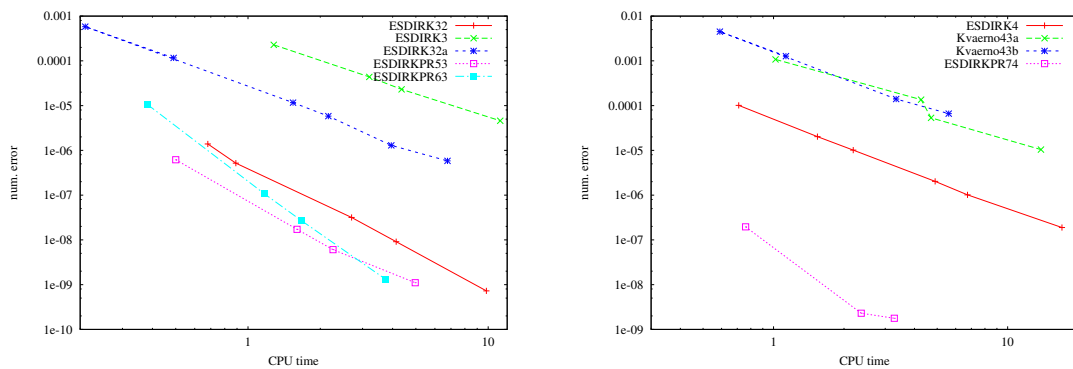


Figure 6: The solution of the index-2 DAE with adaptive timestep control: third order methods (left) and fourth order methods (right)

Next we solve the index-2 DAE (7) with an adaptive time step control time interval $[0, 50]$, where we set $\omega = 10$. The numerical results are shown in Figure 6. In the left part we have the third order methods, which behave similar to the previous simulation with constant step sizes. Again, we have the situation that the index-2 methods perform better than the others. Moreover, the new methods ESDIRK53PR and ESDIRK63PR are more effective than ESDIRK32. The same situation can be observed for the fourth order methods. Here the new ESDIRK74PR method is the most effective one.

References

- [1] E. Hairer and G. Wanner, *Solving ordinary differential equations. II: Stiff and differential-algebraic problems*, Springer Series in Computational Mathematics, vol. 14, Springer-Verlag, Berlin, 1996.

- [2] C. A. Kennedy and M. H. Carpenter, *Additive Runge-Kutta schemes for convection-diffusion-reaction equations*, Applied Numerical Mathematics **44** (2003), 139–181.
- [3] A. Kværnø, *Singly diagonally implicit Runge-Kutta methods with an explicit first stage*, BIT Numerical Mathematics **44** (2004), no. 3, 489–502.
- [4] C. Lubich, *Linearly implicit extrapolation methods for differential-algebraic systems*, Numer. Math. **55** (1989), 197–211.
- [5] J. Rang and L. Angermann, *Remarks on the differentiation index and on the perturbation index of non-linear DAEs*, Mathematik-Bericht 2005/3, Institut für Mathematik, TU Clausthal, 2005.
- [6] J. Rang, *An analysis of the Prothero–Robinson example for constructing new adaptive ESDIRK methods of order 3 and 4*, Informatik-Bericht 2014-06, TU Braunschweig, Braunschweig, 2014, URL: <http://www.digibib.tu-bs.de/?docid=00056090>.
- [7] J. Rang, *The Prothero and Robinson example: Convergence studies for Runge–Kutta and Rosenbrock–Wanner methods*, Informatik-Bericht 2014-08, TU Braunschweig, Braunschweig, 2014, URL: <http://www.digibib.tu-bs.de/?docid=00057194>.

2.6 A component framework for the parallel solution of the incompressible Navier-Stokes equations

Ansprechpartner: Joachim Rang
 EMail: j.rang@tu-bs.de
 Telefon: 0531/391-3007

Many physical or engineering problems can be described with partial differential equations, such as the simulation of time-dependent laminar flows, which can be described by Navier–Stokes equations. The accurate and fast solution of these equations is the core of many numerical simulations of complex processes in nature and industry. The discretisation in space and time is needed for the computation of the solution. In the case of the incompressible Navier–Stokes equations often an inf–sup stable finite element method is used.

Many simulations of incompressible flows use explicit or simple implicit time-stepping schemes. We concentrate in this project on implicit Runge–Kutta methods which are appropriate for laminar flow simulations and which avoid the nasty Courant–Friedrichs–Lewy (CFL) condition. Moreover a high order of convergence can be achieved (see [3, 4]). But these methods need a high computational effort, since in every timestep a nonlinear system of dimension ns has to be solved, where n is the dimension of the problem and s is the number of internal stages of the Runge–Kutta method. In the last decades several papers have discussed the efficient solution of the nonlinear or linear equations. Here we use a transformation from Butcher [2] and Bickart [1] of the coefficient matrix of the Runge–Kutta method. If a simplified Newton method is applied this splitting leads to s complex valued systems of dimension n . These nonlinear systems can be solved directly with the help of LU-decompositions and back- and forward substitutions. But here we have to store s complex LU-decompositions. Therefore we use a parallel framework where each node solves one of the s linear systems.

Therefore the implementation is based on the Component Template Library (CTL) which supports the easy development of distributed as well as parallel applications. This is a C++ template library using template meta-programming to hide as many as possible technical details from the programmer. It has been successfully applied in computational applications such as multi-physics simulation, multi-scale simulation, stochastic finite element analysis and optimisation. The framework described in this project was parallelised with only small changes to an already existing serial code by defining a component interface for the linear solver and by outsourcing this time expensive part to parallel working software components (see [4]).

In our first example of the incompressible Navier–Stokes equations the right-hand side f , the initial condition u_0 and the non-homogeneous Dirichlet boundary conditions are chosen such that

$$\begin{aligned} u_1(t, x, y) &= \sin(t)(y^2 + x), \\ u_2(t, x, y) &= \sin(t)(x^2 - y), \\ p(t, x, y) &= \exp(-t)(x + y - 1) \end{aligned}$$

is the solution of the incompressible Navier–Stokes equations. Moreover we set $Re = 1$, $\Omega = (0, 1)^2$ and solve the problem in the time interval $(0, 1/10]$. We use the Q_2/P_1^{disc} discretisation on a uniform mesh which consists of squares with an edge length $h = 1/512$. Note that for any t the solution can be represented exactly by discrete functions. Hence, all occurring errors will result from the temporal discretisation. As time steps we use $\tau = \frac{16}{10 \cdot 2^k}$, $k = 0, \dots, 6$. The numerical results are presented

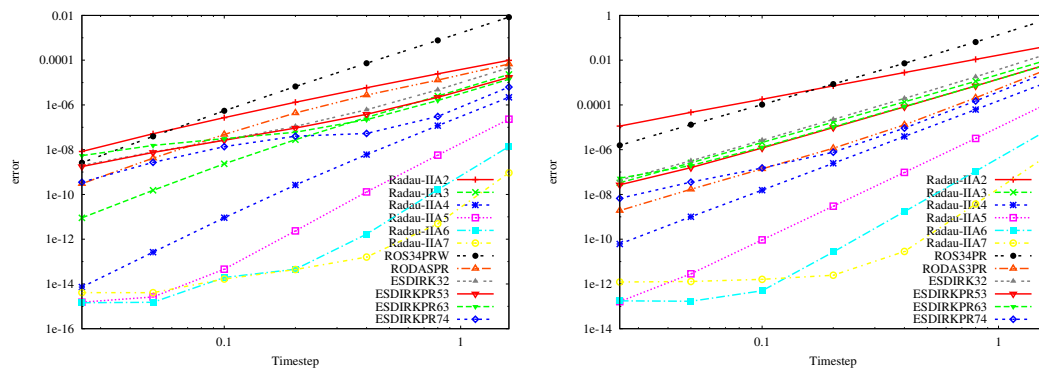


Figure 7: τ versus error: velocity u (left) and pressure p (right)

in Figure 7. It can be observed that the higher order Radau-IIA methods compute the numerical solution more effectively than the DIRK and ROW methods. The Radau-IIA methods have the advantage that the convergence order for the pressure component equals the stage order s . Therefore we get a much faster convergence than for the DIRK and ROW methods.

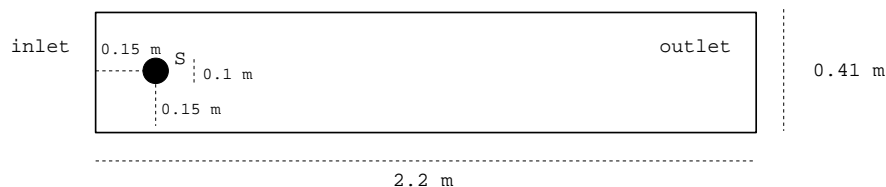


Figure 8: Flow around a cylinder, the channel with the cylinder

The flow around a cylinder which will be considered was defined as a benchmark problem in [5]. Figure 8 presents the flow domain. The right hand side of the Navier–Stokes equations is $f = 0$, the final time is $\bar{t} = 8$, and the inflow and outflow boundary conditions are given by

$$u(t, 0, y) = u(t, 2.2, y) = 0.41^{-2} \sin(\pi t/8)(6y(0.41 - y), 0) \text{ m s}^{-1},$$

for $0 \leq y \leq 0.41$. On all other boundaries, the no-slip condition $u = 0$ is prescribed. The Reynolds number of the flow, based on the mean inflow, the diameter of the cylinder and the prescribed viscosity $\nu = 10^{-3} \text{ m}^2 \text{ s}^{-1}$ is $0 \leq Re(t) \leq 100$.

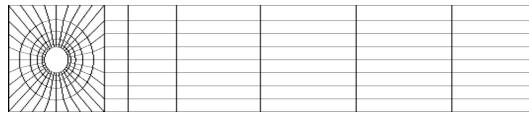


Figure 9: Flow around a cylinder, the coarsest grid (level 0)

The coarsest grid (level 0) is presented in Figure 9. All computations are carried out on level 4 of the spatial grid refinement resulting in 107,712 velocity d.o.f. and 39,936 pressure d.o.f.

In this project we take as benchmark value the difference of the pressure between the front and the back at the cylinder at the final time $p(8, 0.15, 0.2) - p(8, 0.25, 0.2)$. We apply all methods with an adaptive

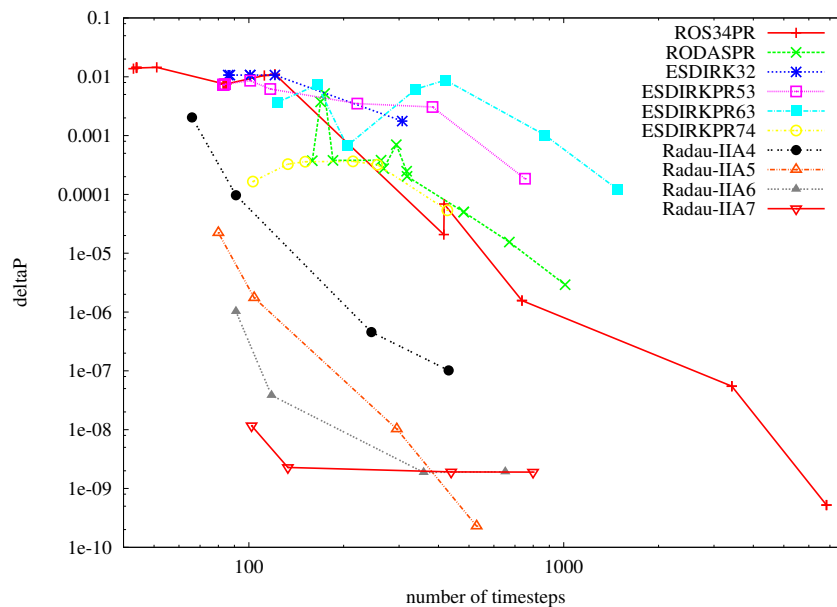


Figure 10: number of timesteps versus error: pressure difference

timestep control. For the computation for the next timestep we use the PI-Controller (see [3] and [4]). In the case of the Radau-IIA methods we use embedded formulas which are introduced in [3]. In Figure 10 we present the numerical results and plot the number of timesteps against the numerical error, because it is difficult to compare the computing time of these methods. In the case of the Radau-IIA methods the linear systems are solved in parallel, i. e. we use s cores, where s is the number of internal stages, and in the case of DIRK and ROW methods no parallel approach is used. It can again be observed that the higher order Radau-IIA methods need less timesteps than our DIRK and ROW methods to reach the same accuracy. In our experience the computing time for one timestep is longer in the case of the Radau-IIA methods, but we need less of them. Hence, for the computations in this paper the

Radau-IIA methods are much more effective than the DIRK and ROW methods.

References

- [1] T. A. Bickart, *An efficient solution process for implicit Runge-Kutta methods.*, SIAM J. Numer. Anal. **14** (1977), 1022–1027 (English), [doi:10.1137/0714069](https://doi.org/10.1137/0714069).
- [2] J. Butcher, *On the implementation of implicit Runge-Kutta methods.*, BIT **16** (1976), 237–240 (English), [doi:10.1007/BF01932265](https://doi.org/10.1007/BF01932265).
- [3] J. Rang, *Adaptive timestep control for fully implicit Runge-Kutta methods of higher order*, Informatik-Bericht 2014-03, TU Braunschweig, Braunschweig, 2014, URL: <http://www.digibib.tu-bs.de/?docid=00055783>.
- [4] J. Rang and R. Niekamp, *A component framework for the parallel solution of the incompressible Navier-Stokes equations with Radau-IIA methods*, Informatik-Bericht 2014-07, TU Braunschweig, Braunschweig, 2014, URL: <http://www.digibib.tu-bs.de/?docid=00056708>.
- [5] M. Schäfer and S. Turek, *The benchmark problem "Flow around a cylinder"*, Flow Simulation with High-Performance Computers II (E. Hirschel, ed.), Notes on Numerical Fluid Mechanics, vol. 52, Vieweg, 1996, pp. 547–566.

2.7 Prediction of damage in bridge structures

Ansprechpartner: Bojana Rosić
 EMail: bojana.rosic@tu-bs.de
 Telefon: 0531/391-3016

Concrete is composite material made from the cement paste and granulates whose mechanical behaviour is characterised by microcracking which further leads to damage. To prevent early deterioration, there is high necessity to detect, localise, and quantify the structure damage given noisy measurement data. Once this step is achieved one is able to predict the life time of structure.

In cooperation with Dr. Julien Waeytens, the French institute of science and technology for transport development and networks, the project work is settled to identify the concrete damage due to vehicle overloading on the bridge. The material model is taken to be the isotropic elastic damage described by tensile and compressive damage variables according to [1, 2]. The former damage variable accounts for microcracks created in the direction of loads, whereas the later one describes slightly slower damaging phenomena which happen in the perpendicular direction to the excitation.

A simplified model of a 2D concrete beam with a single horizontal steel bar is considered as shown in Fig. 11. The steel bar and the concrete are supposed perfectly adherent, and further decomposed into five sections described by a constant Young's modulus and a constant value of the steel bar cross section. The beam is instrumented with fourteen strain sensors, seven on the upper and seven on the bottom part of the beam, which can monitor the traffic-induced strain responses of the beam. The strain is measured over a period of time, and collected into the temporal data series, which further allow the determination of the dynamic moving loading, and hence detection of the damage in the structure.

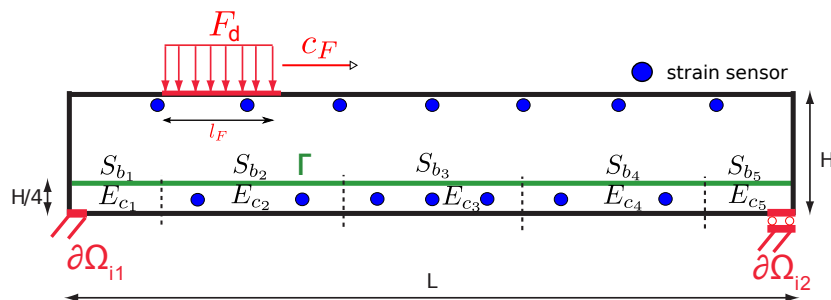


Figure 11: Schematic representation of reinforced concrete beam

For the identification purposes two kinds of approaches are used: the Tikhonov regularisation and the ensemble Kalman filter (EnKF)

Bayes formula. The first procedure is fully deterministic and has for a goal to regularise the ill-posed problem in a least squares sense by penalising the solutions of large norm. On the other side, the EnKF belongs to a family of Bayesian particle like approaches which update the prior probability distributions of unknown parameters with the help of the measurement data and the linear approximation of Bayes rule. In this case 'regularisation' process encounters experts knowledge into the estimation via so co called prior probability distributions.

To solve the Tikhonov minimization problem at a low computation cost, the gradient method with the steepest descent direction obtained by the adjoint approach is utilised. This corresponds to a backward elastodynamics problem whose final conditions vanish. Hence, at each iteration the direct and adjoint problems are solved by taking the control parameters from the previous iteration. Given the direct and adjoint states, the functional gradient is computed. Lastly, the control parameters are updated. The starting values are taken to be the values characterising undamaged material.

In the probabilistic framework, the identification of material parameters is done by assuming all of unknown quantities to be positive definite lognormal distributions with the mean equal to the deterministic values, and variance of 4% of the mean. The estimation is performed with the help of the EnKF with 100 samples and whole time series of measurements. Before the EnKF identification procedure, the parameter and the measurement are transformed to the standard Gaussians with the help of the anamorphosis function, see Fig. 12.

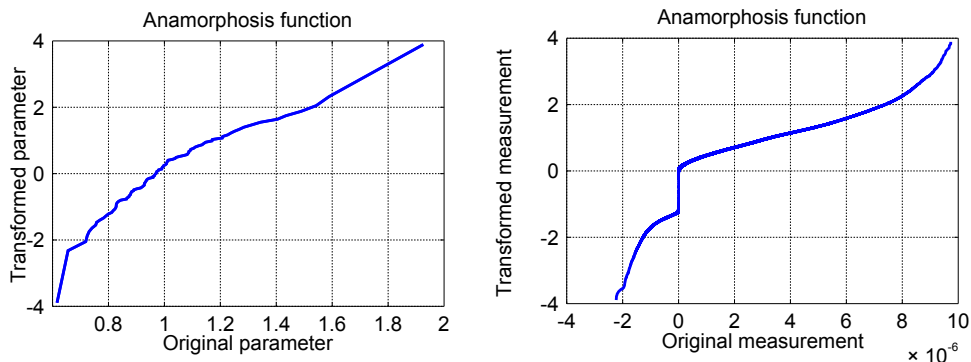


Figure 12: The transformation of non-Gaussian parameters to Gaussian variables

The transformation is done locally for each unknown parameter and for each measurement point. After assimilation, the posterior distributions of the material parameters are obtained, see Fig. 13. To compare these results with the deterministic approach, the mode is selected as representative. According to results shown in Tab. 3, both of approaches are able to detect and localize the concrete damage in the subdomain 3.

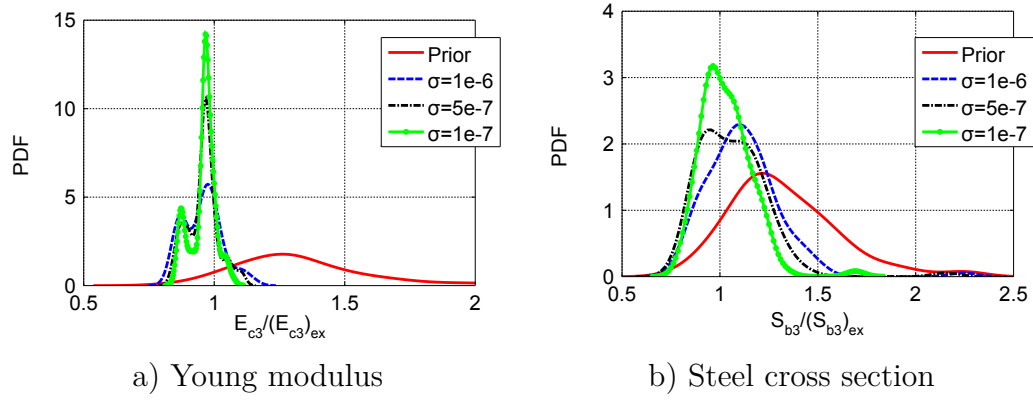


Figure 13: Identification of material parameters in section 3 by probabilistic approach

The Young's modulus is estimated with an error of 8% in the deterministic case and 3% in the probabilistic approach. Concerning the steel bar, Tab. 4 shows that both of approaches do not succeed in properly identifying the reduction of the cross section in the interval 3. In Fig. 13, the posterior distributions of Young modulus E_{c3} and steel bar cross section S_{b3} are compared for different values of the measurement noise σ . As depicted, the posterior variances of both of parameters are smaller than the prior ones-the prior uncertainty is reduced. The reduction is not so much influenced by a measurement noise. However, the uncertainty reduction of Young's modulus is stronger than the corresponding one for the steel bar cross section.

Parameter	$\sigma = 10^{-7}$		$\sigma = 5 \cdot 10^{-7}$		$\sigma = 10^{-6}$	
	D	P	D	P	D	P
$E_{c1}/(E_{c1})_{ex}$	0.96	1.02	1.	1.08	0.99	1.07
$E_{c2}/(E_{c2})_{ex}$	1.	1.06	1.	1.06	1.	0.94
$E_{c3}/(E_{c3})_{ex}$	0.92	0.97	0.85	0.97	1.16	0.98
$E_{c4}/(E_{c4})_{ex}$	1.	1.	0.95	1.0	1.	1.01
$E_{c5}/(E_{c5})_{ex}$	0.97	1.	1.	1.09	0.99	1.11

Table 3: Updating of the concrete Young modulus - comparison of deterministic (D) and probabilistic (P) approaches with respect to the measurement error σ

Parameter	D		P		D		P	
	D	P	D	P	D	P	D	P
$S_{b1}/(S_{b1})_{ex}$	0.98	1.00	1.	1.02	0.99	1.01	1.01	1.01
$S_{b2}/(S_{b2})_{ex}$	1.	0.88	1.	1.03	1.	1.02	1.02	1.02
$S_{b3}/(S_{b3})_{ex}$	1.25	0.97	1.33	0.95	1.27	1.1	1.01	1.01
$S_{b4}/(S_{b4})_{ex}$	1.	1.05	0.99	1.	1.	1.02	1.02	1.02
$S_{b5}/(S_{b5})_{ex}$	0.99	1.08	1.	1.01	0.99	1.01	1.01	1.01

Table 4: Updating of the steel bar cross sections - comparison of deterministic (D) and probabilistic (P) approaches with respect to the measurement error σ

References

- [1] J. Mazars, *A description of micro and macroscale damage of concrete structures.*
- [2] J. Waeytens and B. Rosic, *Comparison of deterministic and probabilistic approaches to identify the dynamic moving load and damages of a reinforced concrete beam,* Tech. report, Institute of Scientific computing, TU Braunschweig.

2.8 Stochastic non-local models of irreversible behavior

Ansprechpartner: Muhammad Sadiq Sarfaraz
 EMail: m.sarfaraz@tu-bs.de
 Telefon: 0531/391-3004

2.8.1 Motivation

Quasi-brittle materials (e.g. concrete) are intrinsically heterogeneous because they are composed of different constituents that are distributed randomly (in case of concrete: cement, fine aggregates, coarse aggregates, water, and admixtures in complex arrangements. To predict their behavior accurately in a computational framework, one needs to take into account, various scales involved in their composition and their interaction with one another (micro, meso, and macro levels). The importance of taking “interaction among scales” under consideration is substantiated by the following facts [8].

- The size, shape, spatial distribution, volume fraction and properties of the constituents making up the micro structure all have a significant impact on the behavior of the material observed at the macro scale, particularly during material failure.
- external loading applied on the materials at the macro scale might in turn cause changes in the micro structural morphology e.g., void formation and coalescence in metals, cracking in cement matrix and inter-facial transition zones in concrete.
- provides a computational tool to design new materials of which desired macroscopic properties can be fulfilled by adjusting the underlying micro structure which is faster and cheaper in comparison then doing same job physically.

Another key point is to consider the uncertainty in the distribution, geometry and sizes of the different constituents, which results in a stochastic material response. Incorporation of uncertainties helps to understand the significance of variability in input parameters in terms of their influence on some output quantity of interest [1, 7].

2.8.2 Objectives

Based on the motivation presented before, a multiscale framework for quasi brittle materials is to be developed based on:

1. Stochastic non-local models

To describe the behavior of quasi brittle materials on macro scale,

it is proposed to use non-local models [5, 2] that are different from the standard local one in the sense that the properties (or state variables) are dependent on not just one material point rather on a finite area. These models are capable of demonstrating physically realizable results in the case of softening (a characteristic response akin to quasi brittle materials under loading). Moreover it is suggested to consider these models as stochastic in order to reflect uncertainty in the description of material behavior.

2. Updating of coarse scale models

To use the non-local models on a coarse scale, one needs to identify the parameters occurring in their constitutive relations. The standard procedure observed in the literature is to perform some specified loading experiments on a Representative Volume Element (a specimen of material under consideration that is representative of its behavior, independent of the size of structure under consideration) and extract the relevant material properties required for the model [6]. However, in a deterministic framework this only yields point estimates. In case of stochastic material model, this task has to be done in a probabilistic framework using Bayesian inference [9].

An essential requirement for material parameter estimation is to have fine scale (or RVE) experiment data. Since there are no physical experiments to be performed, it is proposed to use sophisticated computational model for meso scale (e.g. a lattice model described in [4]), from which fine scale data can be generated by performing simulations with different loading configurations. To give a stochastic character to fine scale data, the developed meso scale model should allow for randomizing the shape, size, positions and material properties of its constituents (e.g. in case of concrete this would be the random distribution of aggregates, mortar and voids) [1].

3. Adaptive Multiscale framework

Finally, the last task is to develop a multiscale framework that relies primarily on coarse scale stochastic model, however during the course of loading, it might happen that certain regions of computational domain can not be modeled accurately by coarse scale model and one needs to switch to fine scale simulation, broadly speaking this can be done in two ways: by using adaptive mesh refinement (refine mesh in critical region without changing the model) or switching to different model, (possibly fine scale). To identify the *critical* regions some error indicator function is required. In case of adaptive mesh refinement, the error estimation focuses on (broadly

speaking) computing the residual of the governing equation, another advancement in this regard is *Goal oriented error estimators* which focus on reducing error incurred in calculating some quantity of interest (QoI). However in the current framework, the goal is to estimate the error incurred due to usage of erroneous model on the coarse scale, in this case model error estimators are proposed in literature which in our case (loosely speaking) gauge the error in constitutive relations (e.g. relation between stress and strain).

To complete the discussion, there is one more issue regarding coupling fine scale model with the coarse scale. The multiscale framework relies on strong geometric coupling between contributing scales (no scale separation is assumed) for this purpose the framework developed in [4] can be employed. For more information on different coupling procedures kindly refer to [3]

References

- [1] J.-B. Colliat, M. Hautefeuille, A. Ibrahimbegovic, and H. G. Matthies, *Stochastic approach to size effects in quasi-brittle materials*, Comptes Rendus Mécanique **335** (2007), no. 8, 430 – 435, [doi:10.1016/j.crme.2007.06.005](https://doi.org/10.1016/j.crme.2007.06.005).
- [2] R. Desmorat, F. Gatuingt, and F. Ragueneau, *Nonlocal anisotropic damage model and related computational aspects for quasi-brittle materials*, Engineering Fracture Mechanics **74** (2007), no. 10, 1539 – 1560, [doi:10.1016/j.engfracmech.2006.09.012](https://doi.org/10.1016/j.engfracmech.2006.09.012).
- [3] Eckardt and Könke, *Adaptive damage simulation of concrete using heterogeneous multiscale models*, Journal of Algorithms & Computational Technology **2** (2008), no. 2, 275–297, [doi:10.1260/174830108784646661](https://doi.org/10.1260/174830108784646661).
- [4] M. Hautefeuille, J.-B. Colliat, A. Ibrahimbegovic, H. Matthies, and P. Villon, *A multi-scale approach to model localized failure with softening*, Computers & Structures **94–95** (2012), no. 0, 83 – 95, [doi:10.1016/j.compstruc.2011.11.007](https://doi.org/10.1016/j.compstruc.2011.11.007).
- [5] M. Jirásek, *Nonlocal models for damage and fracture: Comparison of approaches*, International Journal of Solids and Structures **35** (1998), no. 31-32, 4133 – 4145, [doi:10.1016/S0020-7683\(97\)00306-5](https://doi.org/10.1016/S0020-7683(97)00306-5).
- [6] R. Mahnken, *Identification of material parameters for constitutive equations*, John Wiley & Sons, Ltd, 2004, [doi:10.1002/0470091355.ecm043](https://doi.org/10.1002/0470091355.ecm043).

- [7] H. Matthies and B. Rosić, *Inelastic media under uncertainty: Stochastic models and computational approaches*, IUTAM Symposium on Theoretical, Computational and Modelling Aspects of Inelastic Media (B. Reddy, ed.), IUTAM BookSeries, vol. 11, Springer Netherlands, 2008, pp. 185–194 (English), [doi:10.1007/978-1-4020-9090-5_17](https://doi.org/10.1007/978-1-4020-9090-5_17).
- [8] V. P. Nguyen, M. Stoven, and L. J. Sluys, *Multiscale continuous and discontinuous modeling of heterogeneous materials: A review on recent developments*, *Journal of Multiscale Modelling* **03** (2011), no. 04, 229–270, [doi:10.1142/S1756973711000509](https://doi.org/10.1142/S1756973711000509).
- [9] O. Pajonk, B. V. Rosić, and H. G. Matthies, *Sampling-free linear bayesian updating of model state and parameters using a square root approach*, *Computers & Geosciences* **55** (2013), no. 0, 70 – 83, Ensemble Kalman filter for data assimilation, [doi:10.1016/j.cageo.2012.05.017](https://doi.org/10.1016/j.cageo.2012.05.017).

2.9 Adaptive schemes for stochastic PDEs

Ansprechpartner: Elmar Zander
 EMail: e.zander@tu-bs.de
 Telefon: 0531/391-3011

In the following results of a project that was conducted together with M. Eigel, C. J. Gittelsohn, and Ch. Schwab shall be summarised. The project was about an adaptive scheme for stochastic elliptic partial differential equations where the operator has a certain affine structure [1, 2].

2.9.1 The stochastic elliptic problem

Let the operator for the linear stochastic elliptic problem be given by an operator of the form

$$\mathcal{A}(\theta) = \mathcal{A}_0 + \sum_{k=0}^{\infty} \theta_k \mathcal{A}_k, \quad (8)$$

where θ_k are independent bounded (a.s.) random variables and the operators \mathcal{A}_k are of the form

$$\mathcal{A}_k = \mathcal{D}' \mathcal{M}_k \mathcal{D} \quad (9)$$

where \mathcal{D} is a differential operator, \mathcal{D}' its dual and \mathcal{M}_k a multiplicative operator. Two examples, that have been used in the project, shall be given below:

- Example 1: The diffusion equation

$$\mathcal{D} = v \mapsto \mathbf{v} = \nabla v \quad \mathcal{M}_k = \mathbf{v} \mapsto a_k \mathbf{v} \quad \mathcal{D}' = \mathbf{v} \mapsto \nabla \cdot \mathbf{v} \quad (10)$$

where a_k is the diffusion coefficient

- Example 2: The equations of linear elasticity

$$\begin{aligned} \mathcal{D} = \mathbf{u} \mapsto \boldsymbol{\epsilon} &= \frac{1}{2} [\nabla \mathbf{u} + (\nabla \mathbf{u})^\top] & \mathcal{M}_k = \boldsymbol{\epsilon} \mapsto \boldsymbol{\sigma} &= \mathbf{C}_k : \boldsymbol{\epsilon} \\ \mathcal{D}' = \boldsymbol{\sigma} \mapsto \operatorname{div}(\boldsymbol{\sigma}) & & & \end{aligned} \quad (11)$$

where $\boldsymbol{\epsilon}$ is the strain tensor, $\boldsymbol{\sigma}$ is the stress tensor

2.9.2 Representation of the stochastic solution

The solution of

$$\mathcal{A}(\theta)u(\theta) = f(\theta) \quad (12)$$

is approximated by a spatial and stochastic Galerkin method which is adaptive in both “dimensions”. The representation of the solution u is given by

$$u(\theta) = \sum_{\mu \in \Lambda} P_{\mu}(\theta) u_{\mu}.$$

Here, $\Lambda \subset \mathcal{I}$ denotes the set of active multiindices (i.e. the set of multiindices the adaptive algorithm decided to be important enough to include into the solution), P_{μ} are polynomials orthogonal with respect to measure induced by the random vector $\theta = (\theta_1, \theta_2, \dots)^{\top}$ and the u_{μ} are spatial functions defined on the mesh \mathcal{T}_{μ} , which depends on the multiindex $\mu \in \Lambda$. The evaluation of the bilinear forms appearing in the weak formulation of (12) is approximated by projection on joint meshes.

2.9.3 Error estimator and refinement strategy

The error estimator consists of three parts

- The residual part η_{μ} , which is determined by the mesh resolution of \mathcal{T}_{μ}
- The projection part ζ_{μ}^{ν} , effected by errors in the projections between different meshes \mathcal{T}_{ν} and \mathcal{T}_{μ}
- The part δ_{μ} , caused by neglected multiindices, i.e. the set $\mathcal{I} \setminus \Lambda$

The refinement strategy seek equilibrate errors by either

- Spatial refinement of meshes \mathcal{T}_{μ} belonging to active multiindices $\mu \in \Lambda$
- Selection of new multiindices not yet in the active set Λ . The newly selected multiindices are assigned a relatively coarse initial mesh \mathcal{T}_0 .

2.9.4 Example problem: linear elasticity

A sample problem was computed for the so called Cook’s membrane: a trapezoidal membrane fastened to a wall on the left with a vertical force acting on it on the right (see Fig. 14 left). The initial mesh used is depicted on the right of Fig. 14. The adaptive algorithm lead to the refined meshes as shown in Fig. 15 (however, the meshes are not shown for all active multiindices in Λ). A convergence plot is shown in Fig. 16, depicting the error, the estimator, the efficiency of the estimator and the number of active multiindices over the total degrees of freedom. It can be seen that the estimator achieves good (i.e. nearly constant) efficiency and the error decreases with approximately the optimal theoretical rate, which could be achieved in the deterministic case.

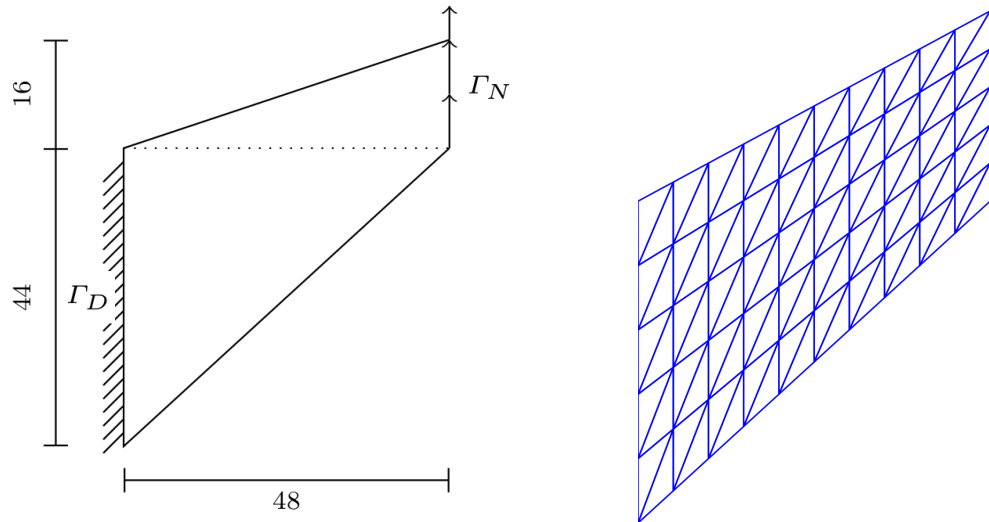
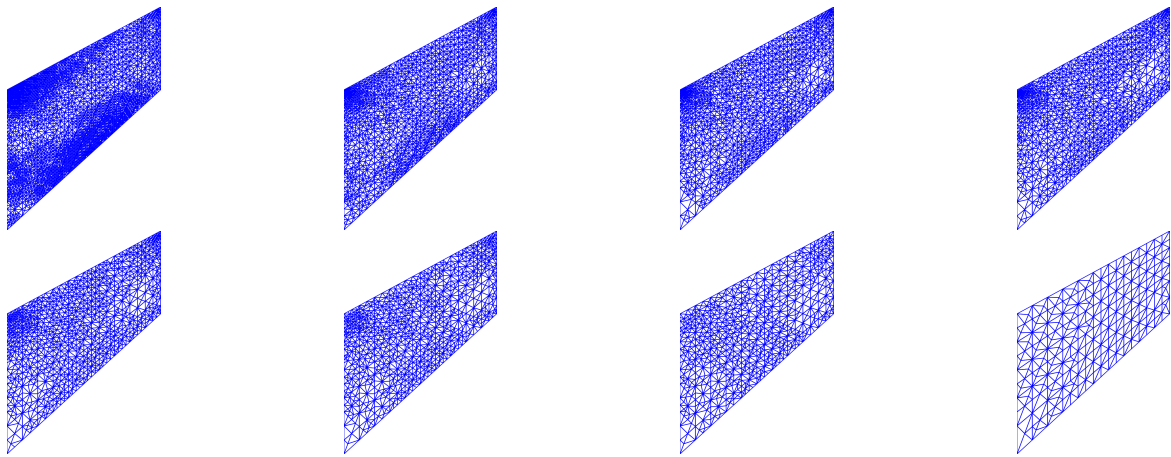
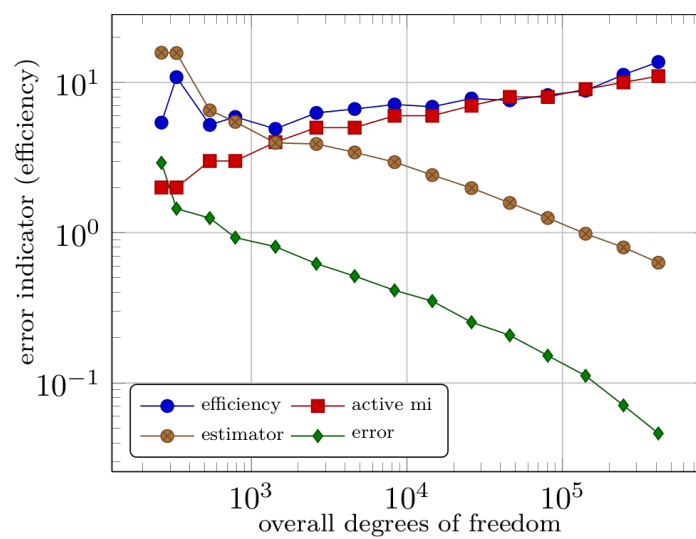
Figure 14: Cook's membrane und initiales mesh \mathcal{T}_0 Figure 15: Adaptively refined meshes for the multiindices (1) , $(0,1)$, $(0,0,1)$, $(0,0,0,1)$, $(0,0,0,0,1)$, $(0,0,0,0,0,1)$, $(0,0,0,0,0,0,1)$, $(0,0,0,0,0,0,0,1)$ 

Figure 16: Convergence of the adaptive method for the Cook's membrane

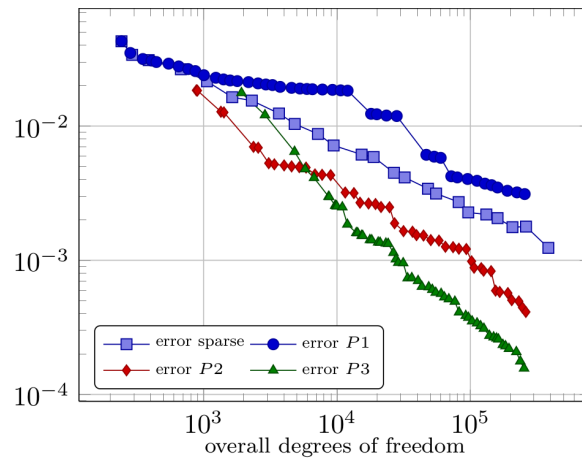


Figure 17: Comparison of the convergence of the method using different meshes with the method using one mesh for linear and higher order FEM

2.9.5 Conclusion

The method proved to be very memory efficient due to very well adapted spatial meshes and multiindex selection. However, due the many necessary projections between differing meshes it is not very runtime efficient. In a subsequent approach, the estimator and adaptive strategy were transferred to a method using only one mesh for all active multiindices. As can be seen in Fig. 17 the method does not attain the efficiency of the fully adaptive method for linear FEM, but performs much better for higher order FEM. Furthermore, it has higher runtime efficiency since no projections are needed, and, as an outlook to future work, is much better amenable to tensor methods.

References

- [1] M. Eigel, C. J. Gittelsohn, C. Schwab, and E. Zander, *Adaptive Stochastic Galerkin FEM*, CMAME (2014), also available as SAM Report 2013-01.
- [2] M. Eigel, C. J. Gittelsohn, C. Schwab, and E. Zander, *A convergent adaptive stochastic Galerkin finite element method with quasi-optimal spatial meshes*, M2AN (accepted), also available as SAM Report 2014-01.

2.10 Hydrological extreme events analysis for flood risk mitigation

Ansprechpartner: Valentina Chiarello
 EMail: valentina.chiarello@dicea.unifi.it
 Telefon: +39-055-2758857 or 0531/391-3005

2.10.1 Introduction

In engineering practice for water resources planning and risk assessment is of primary importance to provide an accurate design flood estimate corresponding to a given risk level. The aim is to implement a new predictive model that may be useful to assess the desired stream flow index (i.e., the flood quantile associated with a given non-exceedance probability, usually expressed in terms of return period) even in ungauged river basins.

2.10.2 Methodologies

According to the Prediction in Ungauged Basin - PUB science initiative promoted by the International Association of Hydrological Science - IAHS [8], hydrologists have developed numerous predictive tools such as empirical models, lumped models, distributed models and statistical regionalizations to predict runoff in ungauged catchments. The estimation of flood frequency quantiles in ungauged river basins and in sites characterized by short or discontinuous time series has been mainly based on regional regression techniques, relating streamflow statistics and geomorphoclimatic basin characteristics. Regional analysis is the classical approach to estimate river flow characteristics at sites where little or no data exists. The knowledge of flood quantiles in ungauged river basins will be provided by two methods: - Use of geostatistic spatial interpolation techniques, which allow estimation of a variable including its uncertainty, like Top-kriging [10] and Residual kriging (RK)[7]; - Use of the distributed and raster-based hydrological balance model MOBIDIC (MOdello di Bilancio Idrologico DIstribuito e Continuo) [3],[4]. These applications of spatial interpolation techniques to regionalization of streamflow regime share a common background idea: both perform a smooth regionalization of streamflow indices seamlessly over the stream network (Top-kriging) or the physiographical space (RK) without identifying groups of hydrologically homogeneous regions. Predict runoff in an ungauged river basins is notoriously a difficult task because the tremendous spatio-temporal heterogeneity of climatic and landscape properties involve significant unknowns and uncertainties. One step of this methodology is the identification of information required for Uncertainty Quan-

tification (UQ) of the model and the application of procedures in order to reduce this uncertainty. The final steps are the quantification of the accuracy of the different models and the comparison of results from the interpolation techniques and from the hydrological model MOBIDIC in order to define the best flood risk management strategy.

2.10.3 Definition of the study area and dataset description

The case study was originally defined by the time series of annual maxima of peaks discharges recorded in the period 1923 - 2011 in several rivers in the Tuscany Region. The proposed Top-kriging procedure was applied to a dataset of 57 runoff gauges with more than 10 years of data to estimate the specific runoff, that is the mean of the annual maxima of peaks discharges time series per unit area. At this point, the Top-kriging interpolation method is applied to the 26 study stream gauges located in the Arno river basin, central Tuscany. *Polygon shape files* of 26 catchments to be used for predictions have been defined. An at-site flood frequency analysis was carried out at each station of the database. Appropriate statistical distributions were fitted to data in order to estimate local flood quantiles corresponding to several return periods. Finally, as specific runoff is considered the flood quantiles corresponding to the 10, 50, 100, 500 year return periods standardized by the basin area to an exponent of 0.65 (the factor $A^{0.65}$) in order to account for the scale effect [1],[5]. The MOBIDIC model required several datasets: the geomorphology of the basin and related hillslope processes are modelling using a Digital Elevation Model (DEM) with 10-m square cells. Information on spatially distributed soil data for soil parameterization and land cover, geology and soil hydraulic properties have been retrieved from existing maps. Input meteorological data were obtained from the regional hydrometeorological monitoring network: Time-series of precipitation (15 min time resolution), air temperature, air humidity, solar radiation and wind speed measured at the gauges inside the sub-basin for recent hydro-meteorological extreme events occurred in the Arno river basin in this last decade 10 year period, 2005 - 2014 have been collected. Finally, water level measurements and stage-discharge relationships in order to obtain discharge data that will be used for model calibration and validation and to assess model performance.

2.10.4 Preliminary results

The implementation of the Top-kriging is based on the package *rtop* of the open source statistical environment R [9]. The sample variogram is estimated as a binned variogram. Given a set of specific parameter, a variogram model is fitted to the estimated binned variogram

through an automatic procedure. The results are validated using a cross-validation procedure in *rtop*, considering the correlation (correlation coefficient=0.74) between observations and predictions. Top-kriging seems to perform better in nested catchments and larger scale catchments but not for headwater or where there is a high variability for neighbouring catchments.

2.10.5 Future works

Up to now, the hydrological model MOBIDIC has been used for water balance evaluation and hydrological forecast in the major basins of Tuscany Region. This model will be applied for the computation and prediction of flood events. Hydrological simulations with specific patterns of rainfall as input for MOBIDIC are required. Particularly, the estimation of rainfall probability distribution needs further investigation. Two different approaches are at the moment under evaluation. One approach is based on the application of the Turning bands method [2] for the synthetic generation of rainfall random fields with specified probability distribution and correlation structure to identify a stochastic space-time rainfall model conditional on rain gauge observations. The procedure for conditioning with respect to point observations is developed in order to provide constraints to Monte Carlo realizations of possible rainfall scenarios. The other approach is based on the use of Copulas with the aim to provide a straightforward approach to the construction of multivariate distribution functions for modelling dependence in space and time [6].

References

- [1] S. A. Archfield, A. Pugliese, A. Castellarin, J. O. Skoien, and J. E. Kiang, *Topological and canonical kriging for design flood prediction in ungauged catchments: an improvement over a traditional regional regression approach?*, Hydrology and Earth System Sciences (2013), no. 17, 1575–1588, [doi:10.5194/hess-17-1575-2013](https://doi.org/10.5194/hess-17-1575-2013).
- [2] R. L. Bras and I. Rodriguez-Iturbe, *Random functions and hydrology*, Courier Corporation, 1985.
- [3] L. Campo, F. Caparrini, and F. Castelli, *Use of multi-platform, multi-temporal remote-sensing data for calibration of a distributed hydrological model: an application in the Arno basin, Italy*, Hydrological Processes (2006), no. 20, 2693–2712, [doi:10.1002/hyp.6061](https://doi.org/10.1002/hyp.6061).

- [4] F. Castelli, G. Menduni, and B. Mazzanti, *A distributed package for sustainable water management: a case study in the Arno basin*, The Role of Hydrology in Water Resources Management (Proceedings of a Symposium Held on the Island of Capri, Italy, October 2008), IAHS Publ. (2009), no. 327, 52–61.
- [5] K. Chokmani and T. Ouarda, *Physiographical space-based kriging for regional flood frequency estimation at ungauged sites*, Water Resources Research **40** (2004), no. W12514, doi:10.1029/2003WR002983.
- [6] B. Gräler and E. Pebesma, *The pair-copula construction for spatial data: a new approach to model spatial dependency*, Procedia Environmental Sciences **7** (2011), 206–211.
- [7] M. K. Nezhad, K. Chokmani, T. B. M. J. Ouarda, M. Barbet, and P. Bruneau, *Regional flood frequency analysis using residual kriging in physiographical space*, Hydrological Processes **24** (2010), 2045–2055, doi:10.1002/hyp.7631.
- [8] M. Sivapalan, K. Takeuchi, S. Franks, V. Gupta, H. Karambiri, V. Lakshmi, X. Liang, J. McDonnell, E. Mendiondo, P. O’Connell, T. Oki, J. Pomeroy, D. Schertzer, S. Uhlenbrook, and E. Zehe, *IAHS Decade on Predictions in Ungauged Basins (PUB), 2003-2012: Shaping an exciting future for the hydrological sciences*, Hydrological Sciences Journal **48** (2003), no. 6, 857– 880, doi:10.1623/hysj.48.6.857.51421.
- [9] J. O. Skoien, *rtop: Interpolation of data with variable spatial support*, 2014, R package version 0.3-45, URL: <http://CRAN.R-project.org/package=rtop>.
- [10] J. O. Skøien, R. Merz, and G. Blöschl, *Top-kriging-geostatistics on stream networks*, Hydrology and Earth System Sciences **10** (2006), no. 2, 277–287.

2.11 A fault detection algorithm for an alternate aerobic/anoxic cycle nitrogen removal process.

Ansprechpartner: Emanuele El Basri
 EMail: emanuele.elbasri@unifi.it or e.el-basri@tu-bs.de
 Telefon: +39-328-4635177 or (+49) 0531/391-3009

2.11.1 Introduction.

It is increasingly difficult to process municipal reject water by means of conventional wastewater treatment plants, given its increasing imbalance between the carbon and nitrogen fractions. There is now a consolidated trend of a decreasing COD¹ load and an increasing reduced nitrogen content, mostly in the ammonia form. For this reason many municipal wastewater treatment plants (WWTPs) are being retrofitted by changing their process flow-sheet in order to make nitrogen removal their primary goal. One efficient way of improving the efficiency of existing small-to-medium WWTPs is to change their operation into a sequence of alternating aerobic/anoxic cycles by switching on and off the aeration in the oxidation tank. The cheapest way of controlling the aeration switch consists in monitoring the Oxidation Reduction Potential (ORP), whose value is related to the ammonium-N content. The principle is the same as in Sequencing Batch Reactors (SBR), with the difference that in this case the switching is applied to a continuous-flow reactor. During the oxidation phase NH_4^+ is oxidized to nitrite (NO_2^-) and then to nitrate (NO_3^-), and the ORP signal rises to positive values until it stabilizes when all the NH_4^+ has been oxidized. At this point the aeration is switched off and the denitrification phase begins, reducing, provided enough organic carbon is available, the oxidized nitrogen (NO_2^- and NO_3^-) just produced. The ORP signal has been largely used to control the process [8], however the limited reliability of the ORP probe has also been reported [3]. With the growing availability of reliable ion-specific probes, the direct measurement of reduced (NH_4^+) and oxidized (NO_x^-) nitrogen is now a viable alternative to ORP, provided the sensor is kept in good order and that its malfunctioning is promptly detected.

2.11.2 Motivation.

Sophisticated sensors such as Ion-Specific Electrodes (ISE) are essential for a precise control policy, but they require careful maintenance. A monitoring system including a fault detection device is instrumental for

¹Chemical Oxygen Demand: expressed in [mg O₂/L] is an indirect measurement of the organic content in wastewater. It represents the amount of oxygen required to chemically oxidise the organic materials using dichromate in an acid solution.

a successful management. The device should also be capable of discriminating a sensor failure to a process anomaly, such as overload or toxic spillage. Hence the need to design a smart fault detection algorithm with these capabilities. Generally, the Fault Detection and Isolation (FDI) algorithms can be divided into three main categories [14]: quantitative model-based methods, qualitative knowledge-based methods and process history-based methods. Of these three approaches, the latter will be followed here, based on the consideration that the vast majority of the FDI approaches rely on a data-mining approach, in which the features of the fault are directly extracted from the process history data. The features can then be processed by non-statistical methods, such as neural networks (NN), principal component analysis (PCA) [12] or partial least squares (PLS), or by a combination of them [4, 7, 13]. PCA is a simple, non-parametric method widely used to emphasize the informative content of a large number of variables, where the information may be masked by noise and data cross-correlation. The PCA provides a linear transformation of the original variables into a new set of orthogonal variables, called Principal Components (PCs), converting a data-rich and information-poor data set into new data for which the information to data ratio is higher. As such, PCA can be used for data dimension reduction. PCA has been widely used in the context of WWTP fault detection, see [15, 2]. Over the years many solutions have been proposed for adapting the PCA algorithm to the varying process conditions. A dynamic version of PCA (DPCA) was proposed by [10] in which a set of time-shifted PCAs is performed for each new sample until the auto- and cross-correlations are minimized and the number of relevant PCs stabilizes. A similar approach can be found in [11], where for each new sample the PCA is performed on the whole dataset, recursively updating both the number of significant PCs and the statistical thresholds. Other methods involve the unfolding (hence the name U-PCA) of the dataset, typically a three-way matrix, showing good results in continuous [5] and transitional processes [6]. Other methods propose the introduction of a moving window to update the reference model [1]. The aim of this work is to develop a new fault detection (FDI) algorithm for alternate aerobic/anoxic cycle waste-water processes for nitrogen removal. The proposed FDI algorithm will be based on an adaptive version of the PCA and will monitor the data produced by the ammonia and nitrate probes deployed in the oxidation tank. The adaptation of the reference system is required by the time-varying nature of the WWTP processes and is achieved by means of a moving window updating system.

2.11.3 Implementation.

Considering the alternating nature of the process operations, the algorithm has been split in two parts, each supervising one phase (aerobic and anoxic). Though they are based on the same principle, they require an individual calibration. First, a preliminary screening is performed on the raw signals in order to detect gross malfunctions such as data interruptions, spikes, anomalous steady measurements and an out-of-range duration of the phases. These malfunctions are basically sensor faults and, being self-explanatory, are easily detected in this preliminary screening. The phases that pass this first filtering are examined for process-related anomalies which escaped the previous simple checks. To this end a PCA-based method has been developed. For each phase both the ammonia and the nitrate signals are parametrized to extract four parameters: the two average concentrations and their rates over the phase duration. These parameters are then processed through PCA and projected onto a reference space from which two control charts, based on the Hotelling's T^2 and Q statistics [9], are used to identify a possible deviation from the normal conditions. If the scores produced by the tested parameters result higher than the respective thresholds in both statistics, then the corresponding phase is reported as a fault, otherwise it is considered "normal" and its parameters are used to update the reference space.

The performance of the algorithm was assessed by comparing the detected anomalies to the fault events actually observed in the historic plant record. The results, considering only phases that are interested by the PCA-based part of the algorithm, are not very satisfactory. However, adding up the performance of the preliminary screening on the signal, the detection success increases dramatically, since the preliminary screening deals with the gross faults, leaving the process anomalies, which typically involve multiple consecutive aerobic and anoxic phases, to be detected by the subsequent PCA analysis. Fig. 18 shows an example of a combined fault detection where both the pre-screening and the PCA parts are active at different times.

The time-scale of the algorithm is very fine, investigating one phase at the time, and this is likely to produce differing responses for two consecutive phases, one of which may yield a positive and the other a negative response. However, using a more coarse time-scale could lead to a lack of definition in the detection task. Thus it makes sense to combine the phases that are logically connected and to evaluate this as a whole event. It was observed that considering as successfully identified the fault events for which over half of the phases are classified as fault, the algorithm proves to have excellent detection performances raising

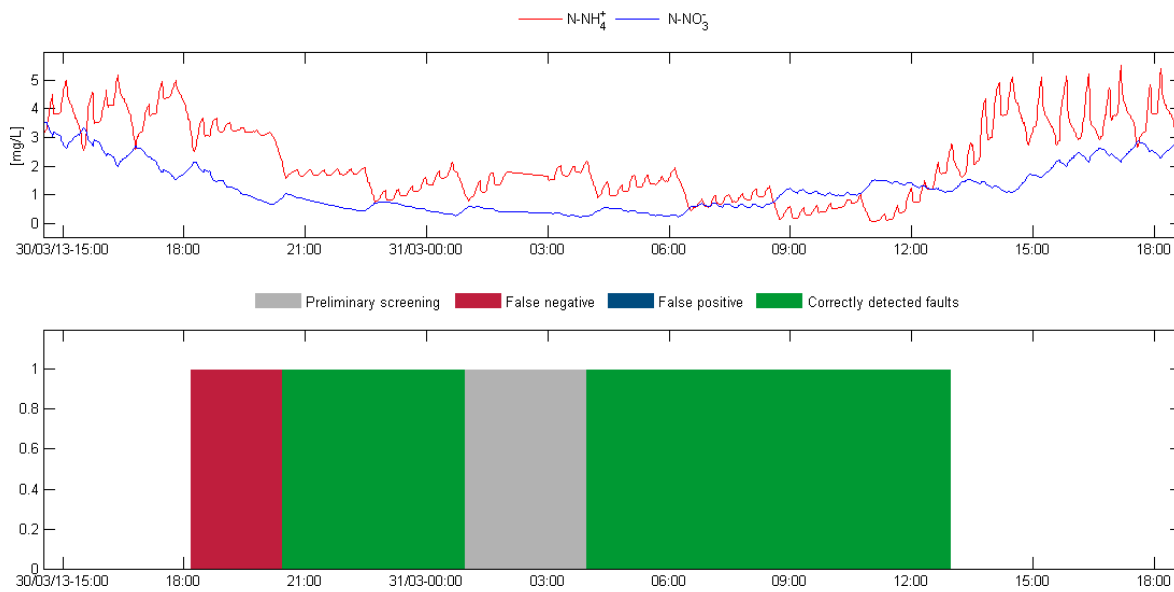


Figure 18: An example of the detection performance of the algorithm. The phases containing faults identified by the preliminary screening are indicated in gray, while in green are detected the faulty phases identified by the PCA-based part of the algorithm. The unidentified faults (false negatives) are presented in red and the false positives in blue.

multiple alarms during long process faults events that lead to the correct identification of all the process anomalies observed in the analysed period.

2.11.4 Future Work.

The proposed method will be extended to other common measurements of WWTPs. This will allow to build an improved inferential model and provide a better characterization of the process anomalies, eventually leading to more reliable detection performances. Also, a Bayesian approach for the reference model updating will be assessed.

References

- [1] F. Baggiani and S. Marsili-Libelli, *Real-time fault detection and isolation in biological wastewater treatment plants*, *Water Science & Technology* **60** (2009), no. 11, 2949–61, [doi:10.2166/wst.2009.723](https://doi.org/10.2166/wst.2009.723).
- [2] L. Corominas, K. Villez, D. Aguado, L. Rieger, C. Rosén, and P. A. Vanrolleghem, *Performance evaluation of fault detection methods for wastewater treatment processes*, *Biotechnology and Bioengineering* **108** (2011), no. 2, 333–44, [doi:10.1002/bit.22953](https://doi.org/10.1002/bit.22953).
- [3] M. de Gracia, A. Larrea, and M. Fabiyi, *Optimization of the alternate cycling process for nutrient removal in industrial wastewater*

- treatment plants—full scale study*, Proceedings of 86th Annual Water Environment Federation Technical Exposition & Conference, no. 19, Water Environment Federation, Chicago, IL, U.S.A, 2013, pp. 286–296, [doi:10.2175/193864713813667647](https://doi.org/10.2175/193864713813667647).
- [4] M. J. Fuente, D. Garcia-Alvarez, G. I. Sainz-Palmero, and P. Vega, *Fault detection in a wastewater treatment plant based on neural networks and PCA*, 20th Mediterranean Conference on Control & Automation (MED), IEEE, Barcelona, Spain, July 2012, pp. 758–763, [doi:10.1109/MED.2012.6265729](https://doi.org/10.1109/MED.2012.6265729).
- [5] D. Garcia-Alvarez, M. J. Fuente, and L. G. Palacin, *Monitoring and fault detection in a reverse osmosis plant using principal component analysis*, 50th IEEE Conference on Decision and Control and European Control Conference (CDC-ECC), IEEE, Orlando, FL, U.S.A., December 2011, pp. 3044–3049, [doi:10.1109/CDC.2011.6160345](https://doi.org/10.1109/CDC.2011.6160345).
- [6] D. Garcia-Alvarez, M. J. Fuente, and G. I. Sainz-Palmero, *Fault detection and isolation in transient states using principal component analysis*, Journal of Process Control **22** (2012), no. 3, 551–563, [doi:10.1016/j.jprocont.2012.01.007](https://doi.org/10.1016/j.jprocont.2012.01.007).
- [7] P. V. Goode and M.-Y. Chow, *A hybrid fuzzy/neural system used to extract heuristic knowledge from a fault detection problem*, IEEE 3rd International Fuzzy Systems Conference, IEEE, Orlando, FL, U.S.A., July 1994, pp. 1731–1736, [doi:10.1109/FUZZY.1994.343595](https://doi.org/10.1109/FUZZY.1994.343595).
- [8] G. Guglielmi and G. Andreottola, *Alternate anoxic/aerobic operation for nitrogen removal in a membrane bioreactor for municipal wastewater treatment*, Water Science & Technology **64** (2011), no. 8, 1730, [doi:10.2166/wst.2011.755](https://doi.org/10.2166/wst.2011.755).
- [9] H. Hotelling, *Multivariate quality control illustrated by the testing of sample bombsights*, Selected techniques of statistical analysis (O. Eisenhart, ed.), McGraw-Hill, New York, NY, U.S.A., 1947, pp. 113–184.
- [10] W. Ku, R. H. Storer, and C. Georgakis, *Disturbance detection and isolation by dynamic principal component analysis*, Chemometrics and Intelligent Laboratory Systems **30** (1995), no. 1, 179–196, [doi:10.1016/0169-7439\(95\)00076-3](https://doi.org/10.1016/0169-7439(95)00076-3).
- [11] W. Li, H. H. Yue, S. Valle-Cervantes, and S. J. Qin, *Recursive PCA for adaptive process monitoring*, Journal of Process Control **10** (2000), no. 5, 471–486, [doi:10.1016/S0959-1524\(00\)00022-6](https://doi.org/10.1016/S0959-1524(00)00022-6).

- [12] K. Pearson, *On lines and planes of closest fit to systems of points in space*, *Philosophical Magazine* **2** (1901), no. 6, 559–572.
- [13] M. L. Ruiz Ordóñez, G. Sin, X. Berjaga, J. Colprim, S. Puig, and J. Colomer, *Multivariate Principal Component Analysis and Case-Based Reasoning for monitoring, fault detection and diagnosis in a WWTP*, *Water Science & Technology* **64** (2011), no. 8, 1661, [doi:10.2166/wst.2011.517](https://doi.org/10.2166/wst.2011.517).
- [14] V. Venkatasubramanian, R. Rengaswamy, S. N. Kavuri, and K. Yin, *A review of process fault detection and diagnosis*, *Computers & Chemical Engineering* **27** (2003), no. 3, 293–346, [doi:10.1016/S0098-1354\(02\)00161-8](https://doi.org/10.1016/S0098-1354(02)00161-8).
- [15] K. Villez, P. A. Vanrolleghem, C. Rosén, F. Anctil, and C. Duchesne, *Qualitative representation of trends: an alternative approach to process diagnosis and control*, *Water Science & Technology* **57** (2008), no. 10, 1525–32, [doi:10.2166/wst.2008.141](https://doi.org/10.2166/wst.2008.141).

2.12 Numerical Modelling and Optimization of Oscillating Water Column Wave Energy Converters

Ansprechpartner:	Irene Simonetti
EMail:	irene.simonetti@dicea.unifi.it
Telefon:	+39-393-0444704

2.12.1 Introduction

A large variety of Wave Energy Converters (WECs) [6] have been proposed, and among them the Oscillating Water Column (OWC) is one of the only devices to have reached the full scale prototype development stage [1, 11]. The device basically consists of a hollow chamber, open below the water surface, so that the incident and retreating wave respectively pressurizes and de-pressurizes the air, generating a reciprocating airflow which drives self-rectifying air turbines. Optimization is still a crucial point for the commercial-scale diffusion of this technology. Therefore, research at fundamental level is still required. Some specific issues have to be taken into account when selecting a numerical modelling approach for OWC devices, i.e.: (i) vortex and turbulent flow formation in the front wall region; (ii) the possibility of turbulent air flows in the OWC chamber, with the presence of suspended water droplets; (iii) relevant non-linear components of the incident wave field, particularly for shoreline-devices; (iv) spring-like effects of air compressibility may significantly affect the converter dynamics [8]. The major research efforts in the field of OWC numerical modelling are focused on hydrodynamics, i.e. on resolving diffraction and radiation problems around the structure. The aerodynamic domain (i.e. air chamber and ducts) is usually modelled by using the principle of mass conservation and isentropic air compression/decompression processes approximations. The Power Take Off (PTO) is generally introduced as an external damping. The linear wave theory has traditionally been applied to study the interaction between incident waves and OWCs, with the application of simplified models such as the rigid piston model [5] and the uniform pressure distribution model [7]. When the OWC geometry is complex, or a relevant effect of the installation site bathymetry is expected, Finite Element Methods (FEM) or Boundary Element Methods (BEM) [3] are usually applied to compute the OWC hydrodynamic coefficients (added mass and radiation damping). When a proper characterization of viscous effect due to boundary layer separation, wave breaking and turbulence are expected to be relevant, approaches based on potential flow theory are no longer appropriate, and a solution based on Navier-Stokes equations (Computational Fluid Dynamic, CFD) is required. However, the hydrodynamics and aerodynamics of the two-phase system are currently

not yet included in studies using a CFD approach.

2.12.2 Methodology

A state of the art review on OWC technology was performed, with particular focus on the most suited numerical modelling techniques for OWC and on the suitable air turbine types. In early stage of the research activity, a semi-analytical models of the OWC device was developed in Matlab environment in order to: (i) preliminary evaluate the range of values of pressure and air flow in the air chamber for the instrument set up of laboratory experiments; (ii) to select the relevant design parameters to be deeply investigated in a further optimization phase (Figure 19). Aiming to simulate two-phase (air-water) interacting fluids inside the OWC chamber, and to take into account the effects of non linearities as well as that of turbulent flows, Computational Fluid Dynamic (CFD) techniques were adopted to simulate the OWC air chamber behaviour. The model is validated with data from physical tests. Both incompressible and compressible multiphase flow solvers are used, with the aim of evaluating air compressibility scale effects and integrate the small scale laboratory experiments. The CFD model is used to perform a parametric optimization of the OWC geometry within the site-specific sea state context considered adopting, using and hybrid 2D-3D approach to reduce the computational demands of the model [4].

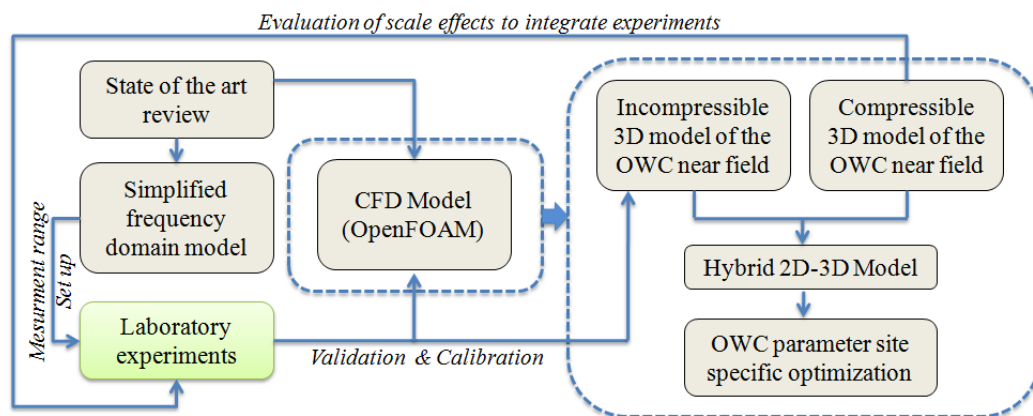


Figure 19: Work flow-chart.

2.12.3 Simplified frequency domain model

A simplified model of a cylindrical OWC, based on linear wave theory, was implemented. The model uses a rigid piston schematization of the OWC inner water surface. The equation of motion of the water surface (Eq. 13) allows to determine the water level and the air pressure inside the chamber.

$$m_w \ddot{z} + z(t)S\rho g + p(t)S = f_e + f_{rad} \quad (13)$$

where m_w is the mass of the rigid piston, ρ is the water density, g is gravitational acceleration, p is the air pressure in the OWC chamber, S is the area of the OWC horizontal cross-section, f_e is the force due to the hydrodynamic pressure caused by the incident wave and f_{rad} is the hydrodynamic force due to the radiated wave produced by the pressure oscillation on the inner free surface.

Compression and decompression of the air are assumed to be isentropic and the model is solved in frequency domain. Regular and irregular incident waves are considered. A stochastic approach was adopted for irregular waves. The fully linear model is able to simulate water level, pressure and air flow inside the OWC chamber and to give preliminary indications about the device wave energy extraction capability (Fig. 20). The effect of different values of the OWC basic geometrical parameters, i.e. the radius and the draught, was tested, as well as the effect of the turbine damping (defined by its rotational speed and diameter). The model has been applied to preliminarily characterize the OWC air chamber pressure and air flow ranges, to assist the choice of the working range of the instruments adopted in physical model testing [9].

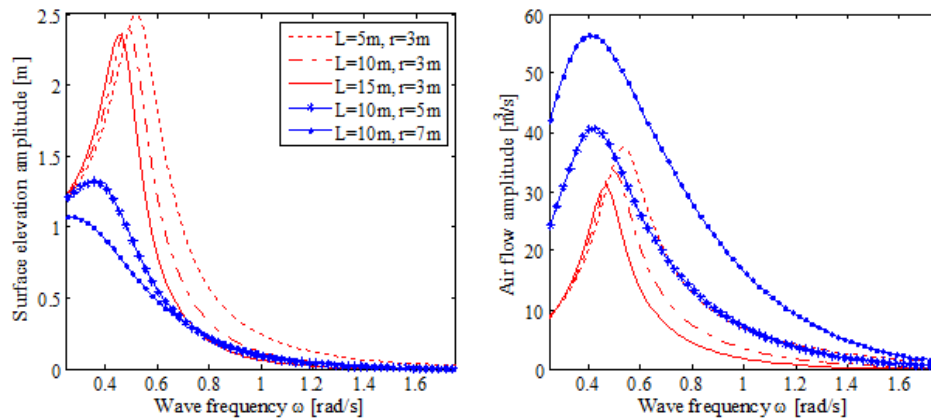


Figure 20: Absolute value of the OWC surface elevation oscillation and air flow amplitude predicted by the simplified frequency domain model (for an incident wave with height 1 m, and turbine rotation speed 100 rad/s).

2.12.4 CFD model in OpenFOAM

The CFD model of the OWC device was implemented within the OpenFOAM framework. Both incompressible (`interFoam`) and compressible (`compressibleInterFoam`) two-phase solvers are used. The solvers use the Volume Of Fluid (VOF) method for free surface tracking, solving Navier-Stokes equations for a single Eulerian fluid mixture of two-phases (i.e. water and air). The discretization of the flow equations is based

on the Finite Volume Method (FVM) with a co-located methodology for unstructured polyhedral meshes with arbitrary grid elements. The simulated OWC geometry corresponds to the one used for the physical tests on a small scale model in Florence University [2]. A numerical wave flume was developed and tested, using comparatively different approaches for wave generation and absorption in order to highlight the strength and the drawbacks of methods in terms of both accuracy on reproducing the wave dynamics and computational demands. The tested approaches are: (i) a specific toolbox (`waves2Foam`) developed as an extension to the `interFoam` solver, in which the hydrodynamic solver is coupled with a relaxation zones approach; (ii) wave generation with a piston wave-maker, simulated imposing a moving wall boundary condition (i.e., dynamic mesh) [10]. Different turbulence models were tested [10], and results of the 3D model are in good agreement with experimental data (relative error lower than 7% for all the considered benchmark parameters) using a k-equation eddy-viscosity Large Eddy Simulation (Figs. 21-22). Both the compressible and the incompressible model results are in good agreement with the small scale laboratory data. Therefore, the numerical model under development constitutes a proper tool to perform extensive parameter investigations, increasing the number of physically studied OWC geometries and wave conditions.

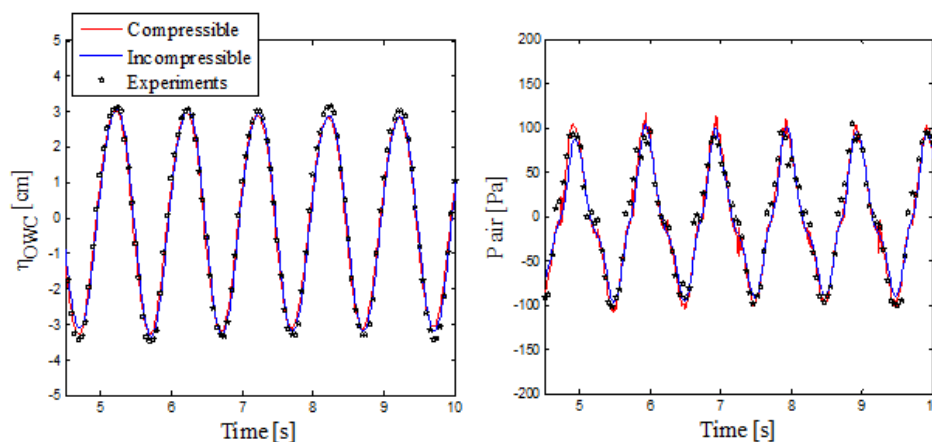


Figure 21: Comparison between experimental and numerical (with compressible and incompressible VOF model in OpenFOAM) results for water surface oscillation and air pressure in the OWC chamber.

2.12.5 Future Work

The use of the compressible model for the assessment of air compressibility scale effects, to integrate data from small scale laboratory experiments, is currently being performed, by simulating the OWC device at different scales. The complete parameter study, aimed to select the optimal OWC geometry and turbine applied damping for maximum energy

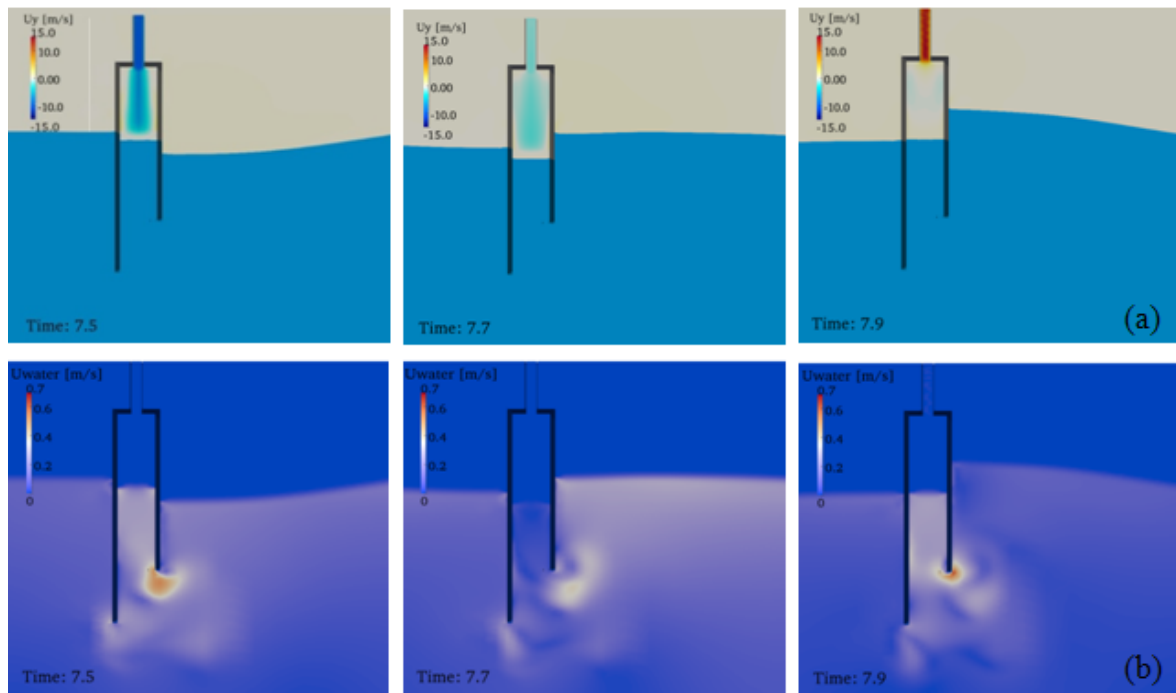


Figure 22: 2D cross-section of vertical component of the air velocity in OWC chamber (a) and water velocity near the OWC chamber (b) simulated with the OpenFOAM model at different time steps during wave propagation.

conversion for a specific wave climate, will be the following steps of the research work.

2.12.6 References

References

- [1] C. B. Boake, T. J. T. Whittaker, M. Folley, and H. Ellen, *Overview and Initial Operational Experience of the LIMPET Wave Energy Plant*, 12th International Offshore and Polar Engineering Conference, vol. 3, 2002, p. 9.
- [2] I. Crema, I. Simonetti, L. Cappietti, and H. Oumeraci, *Laboratory experiments on Oscillating Water Column Wave Energy Converters integrated in a Very Large Floating Structure*, 11th Wave and Tidal Energy Conference, EWTEC2015. Submitted, 2015.
- [3] Y. Delauré and A. Lewis, *3D hydrodynamic modelling of fixed oscillating water column wave power plant by a boundary element methods*, *Ocean Engineering* **30** (2003), no. 3, 309–330, [doi:10.1016/S0029-8018\(02\)00032-X](https://doi.org/10.1016/S0029-8018(02)00032-X).
- [4] H. El Safti, L. Bonakdar, and H. Oumeraci, *A hybrid 2D-3D CFD model system for offshore pile groups subject to wave loading*, 33rd International Conference on Ocean, Offshore and Arctic Engineering OMAE2014, 2014, pp. 1–11.

- [5] D. Evans, *The Oscillating Water Column Wave Energy Device*, Journal of Fluid Mechanics **22** (1978), 423–433.
- [6] A. O. Falcão, *Wave energy utilization A review of the technologies*, Renewable and Sustainable Energy Reviews **14** (2010), 899–918, [doi:10.1016/j.rser.2009.11.003](https://doi.org/10.1016/j.rser.2009.11.003).
- [7] A. O. Falcão and P. Justino, *OWC wave energy devices with air flow control*, Ocean Engineering **26** (1999), 1275–1295.
- [8] A. Sarmiento and A. O. Falcão, *Wave generation by an oscillating surface-pressure and its application in wave-energy extraction*, Journal of Fluid Mechanics **150** (1985), 467–485.
- [9] I. Simonetti, L. Cappiotti, H. El Safti, and H. Oumeraci, *Numerical Modelling of fixed oscillating water column wave energy conversion devices: toward geometry hydraulic optimization*, 34th International Conference on Ocean, Offshore and Arctic Engineering, OMAE2015. Accepted, 2015, pp. 1–10.
- [10] I. Simonetti, L. Cappiotti, G. Manfrida, H. Matthies, and H. Oumeraci, *The use of OpenFOAM as a virtual laboratory to simulate oscillating water column wave energy converters*, International Conference on Computational Methods in Marine Engineering, MARINE2015. Submitted, 2015, pp. 1–12.
- [11] Y. Torre-Enciso, J. Marqués, and L. I. L. D. Aguilera, *Mutriku. Lessons learnt*, 3rd International Conference on Ocean Energy, Bilbao, 2010, pp. 2–7.

2.13 A numerical approach to the dynamics analysis of marine cables

Ansprechpartner: Giovanni Stabile
 EMail: giovanni.stabile@dicea.unifi.it
 Telefon: +39-055-4796306 or +39-333-5273567

2.13.1 Motivation

Long slender cylinders are found in many offshore applications and are the representative system for risers and mooring lines in deep water. The response of this kind of structure due to wave, current and tide loads may be complex, and phenomena such as vortex induced vibrations (VIV), unsteady lock-in, dual resonance, and travelling waves response may occur [18]. The methods used in the literature to solve the response analysis of long slender cylinders can be mainly divided into the following: experimental activities, semi empirical methods, and CFD methods. For more details one may refer to several review articles [1, 4, 17]. In this paper we will focus our attention on CFD methods, which have demonstrated to be a promising way to capture the response of this kind of structure. They can be classified into two different classes:

- Full 3D simulations [12, 2], where the flow is discretized using three-dimensional elements. This approach has the advantage of capturing completely the three-dimensionality of the flow, but even with today's computational resources this is too demanding for the case of long cylinders and for flows with realistic values of the Reynold's number.
- Strip theories where the flow is modelled using bi-dimensional analysis at several different positions along the cable length. The flow at different planes is completely independent [10, 6, 19], and the three-dimensionality is only due to the structural model. This approach is computationally less demanding, and flow with realistic values of Reynold's number can be simulated. The disadvantage is that the three-dimensionality of the flow can not be captured, and forces at different planes have to be interpolated, and it is not easy to find a general way to perform such an interpolation.

The idea is to use the advantages of both methods. The response of the cable is studied only locally on a reduced domain size, which permits the use of a complete three-dimensional analysis with values of the Reynold's number suitable for practical applications. The logical process on which the ROM is based is summarized in Figure 23. A section of the cable, which is already three-dimensional, is subjected to an

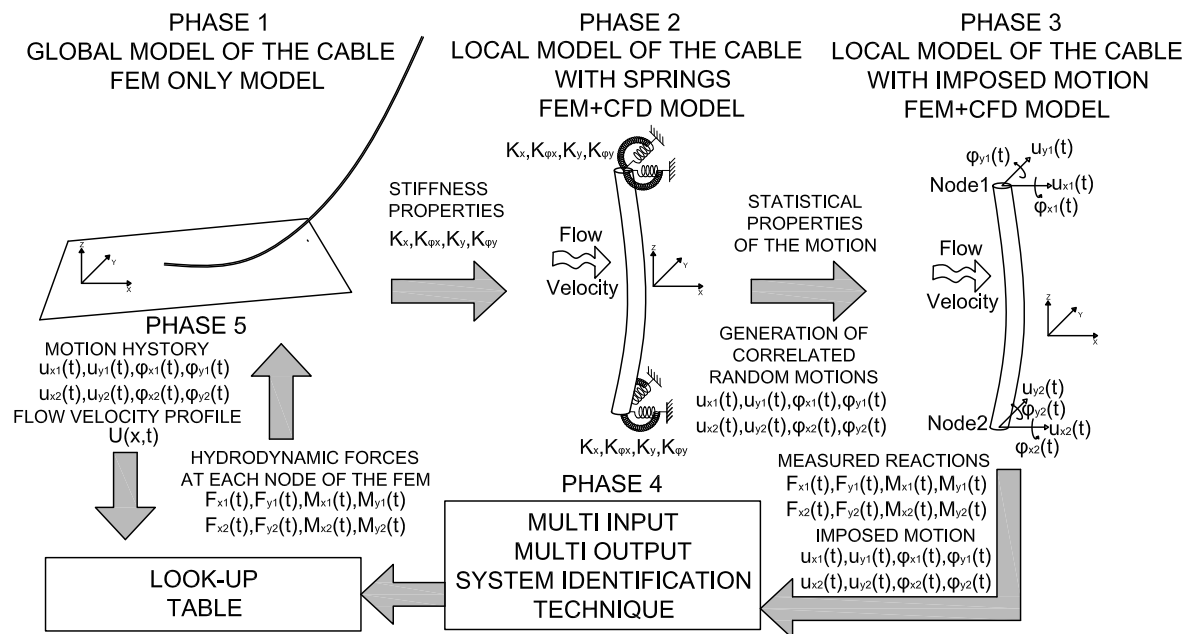


Figure 23: Flowchart of the discussed method

imposed motion with the same statistical characteristics as the response expected in full scale. The statistical characteristics of the motion in full scale could be carried out through full scale measurements (PHASE 3). Since full scale measurements were not available, the statistical properties of the imposed motion have been also obtained through high fidelity simulations on small scale size (PHASE 2). The cable has been retained at both ends with suitable springs which replace the remaining parts of the cable. The stiffness properties of the springs have been deduced from the FEM model in full scale (PHASE 1). It has been assumed that, in small scale, at the ends of the cable only transverse translations and bending rotations are relevant. This assumption does not limit in any way the motion of the cable in full scale which can move with all possible degrees of freedom. It is simply assumed that the fluid forces exerted on the cylinder due to the translation along its axis and due the rotation around its axis can be neglected. Once the statistical properties of the full scale motions are known one can create a random motion for each released degree of freedom. The so created random motions are imposed to the high fidelity small scale model, and the forces are measured (PHASE 3). The results of this analysis, varying the flow velocity and the flow inclination, may be used to feed a system identification technique that can be used to create a look-up table (PHASE 4). Such a look-up table once prepared could be added to any FEM solver. The additional DOFs are only internal and are identified through a system identification technique. At each time step, hydrodynamic forces, can be obtained simply calling the so developed finite element where only the instantaneous characteristics of motion are required.

2.13.2 The coupled problem

The method described in the previous chapter is strongly based on the FSI small scale problem of phases 2 and 3. The coupled problem is here solved using a partitioned strategy with a direct force motion method (DFTM). In general a fluid structure interaction problem is formed by three different sub-problems: the fluid problem, the solid problem, and the mesh motion problem. The structural problem will be henceforth indicated with s while the fluid problem will be indicated with f . The solid problem is governed, in a spatial Lagrangian frame, by the momentum balance equation in terms of Cauchy stresses:

$$\nabla \cdot \sigma + \rho_s(\mathbf{b} - \ddot{\mathbf{u}}) = \mathbf{0} \text{ in } \Omega_s \times [0, T] \quad (14)$$

where σ is the Cauchy stress tensor, ρ_s is the solid density, \mathbf{b} is the body force vector, $\ddot{\mathbf{u}}$ is the acceleration vector. Ω_s is the structural domain, and T is the length of the considered time window. A Newtonian, incompressible, viscous, isothermal and isotropic flow is considered. Since the fluid domain is not static but changing in time due to the deformation of the solid body we need to reformulate the Navier-Stokes equation for incompressible and viscous flows considering the motion of the FSI interface. This is done using an arbitrary-Lagrangian-Eulerian (ALE) [3] framework referenced to a frame moving with a velocity \mathbf{v}_m . What we need to do is to replace inside the convective term the velocity \mathbf{v} with the convective velocity $\mathbf{v}_c = \mathbf{v} - \mathbf{v}_m$, where \mathbf{v}_m is the velocity of the moving part of the domain. The momentum balance equation and the continuity equation, for the fluid domain, can be written in a spatial Eulerian frame as:

$$\begin{aligned} \frac{\partial \mathbf{v}}{\partial t} + (\mathbf{v}_c \cdot \nabla) \mathbf{v} - \nu \nabla^2 \mathbf{v} &= -\frac{1}{\rho_f} \nabla p \quad \text{in } \Omega_f \times [0, T] \\ \nabla \cdot \mathbf{v} &= \mathbf{0} \quad \text{in } \Omega_f \times [0, T] \end{aligned} \quad (15)$$

where \mathbf{v} is the flow velocity vector, t is the time, ν is the flow viscosity, and p is the pressure. Ω_f is the fluid domain, and T is the length of the considered time window. In the present work the solid and the fluid problem are solved using different space discretization techniques. The solid problem is solved using finite elements, while the fluid problem is solved using finite volumes. The mesh motion problem is solved imposing the matching of velocities and stresses at the FSI interface:

$$\begin{aligned} \mathbf{v}_s &= \mathbf{v}_f \text{ on } \partial\Omega_{FSI} \times [0, T] \\ \mathbf{n} \cdot \sigma &= -p\mathbf{n} + 2\nu(\mathbf{n} \cdot \nabla^S) \mathbf{v}_f \text{ on } \partial\Omega_{FSI} \times [0, T] \end{aligned} \quad (16)$$

Algorithm 1 Coupling algorithm

Given: initial time T_0 , length of the simulation T , time step size of the fluid simulation Δt_f , time step size of the solid simulation Δt_s , time step size of the the coupled simulation Δt_c , the tolerance $TOLz$

```

while  $t < T$  do
   $k = 0, \omega^{(0)} = \omega_0$ 
  while  $res_{N+1}^{(k)} < TOL$  do
    if  $k > 0$  then
       $\omega^{(k)} = -\omega^{(k-1)} \frac{res_{N+1}^{(k-1)} \cdot (res_{N+1}^{(k)} - res_{N+1}^{(k-1)})}{\|res_{N+1}^{(k)} - res_{N+1}^{(k-1)}\|^2}$ 
    end if
    Predict fluid velocities at the interface:  $\mathbf{V}_{f,N+1}^{(k)} = P(\mathbf{V}_N^{(k_{max})}, \mathbf{V}_{N-1}^{(k_{max})}, \dots)$ 
    Given  $\mathbf{V}_{f,N+1}^{(k)}$  solve the fluid problem in ALE formulation  $\rightarrow \mathbf{F}_{f,N+1}^{(k)}$ 
    Given  $\mathbf{F}_{f,N+1}^{(k)}$  solve the solid problem  $\rightarrow \mathbf{V}_{S,N+1}^{(k)}$ 
    Evaluate residual  $res_{N+1}^{(k)} = \mathbf{V}_{S,N+1}^{(k)} - \mathbf{V}_{f,N+1}^{(k)}$ 
    Update fluid velocity at the interface  $\mathbf{V}_{f,N+1}^{(k+1)} = \mathbf{V}_{S,N+1}^{(k)} + \omega^{(k)} res_{N+1}^{(k)}$ 
     $k = k + 1$ ;
  end while
   $N = N + 1, t = t + \Delta t_c$ 
end while

```

Figure 24: Coupling Algorithm

where \mathbf{n} is the FSI-interface normal vector, ∇^S is the symmetric part of the gradient operator. The matching of variables at the interface is enforced with an implicit scheme which conserves the energy at the interface. For each time step of the coupled simulation $t_{c,i}$ an iterative cycle on the velocity residual is performed until the achievement of a desired tolerance:

$$\mathbf{res} = \mathbf{v}_{s,i} - \mathbf{v}_{f,N} \leq TOL \quad (17)$$

The iterative scheme is realized using a block Gauss-Seidel procedure reported in Figure 24 [11]. The time step size of the fluid sub-problem may be different to the time step size of the solid sub-problem. The only requirement is that each sub-problem has to be performed the sufficient number of times necessary to reach the time step size of the coupled simulation. Inside the algorithm the term ω is a scalar value obtained by Aitken's relaxation [9]. The procedure will work with any CFD solver and any CSD solver which can be coupled properly, here the solid sub-problem is solved using the FEM solver FEAP [16], while the fluid sub-problem is solved using the FVM solver OpenFOAM [8]. The coupling is realized using the approach of software components and the component template library (CTL) [11] is used as common middleware. Here the features of the FSI solver are reported only briefly, for additional details please refer to [7].

2.13.3 The Fluid Sub-Problem

The fluid computation has been carried out using a large eddy simulation (LES) turbulence model [14]. This approach has demonstrated

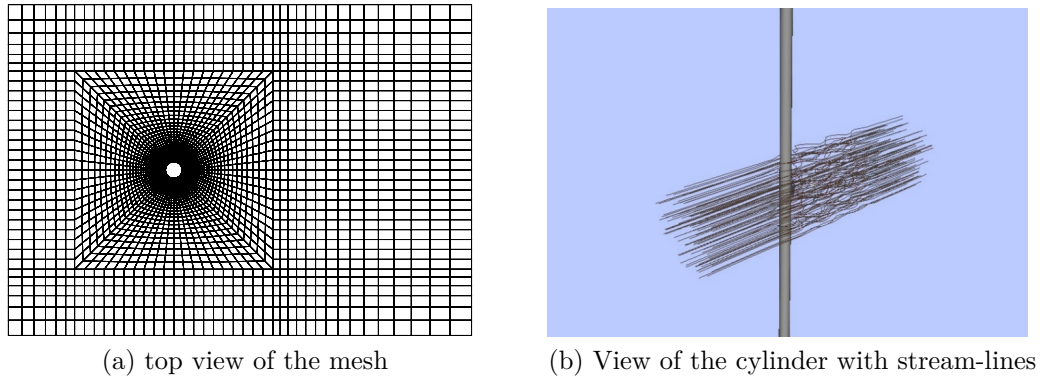


Figure 25: Domain of the simulation

to be particularly suitable to analyse the flow around a circular cylinder especially in the range of Reynold's numbers interesting for practical applications [13]. The sub grid scale model is a k -equation eddy viscosity model. The mesh is represented in Figure 25 and is structured using a polar distributed grid in the proximity of the cylinder and a Cartesian distributed grid in the other regions. The region near to the wall has been refined, and along the vertical direction an equally spaced mesh has been used ($\Delta z \approx D/2$).

The distance of the cylinder from the inlet is equal to $8D$, the distance from the outlet is equal to $15D$, and the domain width is equal to $20D$. The diameter of the cylinder is equal to $D = 0.102\text{m}$, which is a common diameter for mooring line cables available on the market. The domain height is equal to $40D$. The height of the domain has been chosen in order to make the structure slender enough to be modelled using a beam theory. The flow has a constant uniform velocity at the inlet and constant zero pressure value at the outlet. Sides are modelled with slip conditions, and the lower and upper part are modelled as symmetry planes. The PIMPLE algorithm [8] and an Euler implicit scheme with a time step $\Delta t_f = 0.001\text{s}$ are used. The fluid is water with a density of $\rho_f = 10^3\text{kg/m}^3$ and kinematic viscosity of $\nu_f = 1 \times 10^{-6}\text{m}^2/\text{s}$.

2.13.4 The Solid Sub-Problem

Since we are not interested in the accurate modelling of the stresses inside the cylinder but rather on the global response of the cable, the structure has been modelled using a geometrically exact beam element based on [15]. The time integration has been performed using a generalized HHT- α integration scheme [5] which has been demonstrated to be enough accurate for the specific case. The structure has been discretized with 40 equally spaced finite elements with the same spacing used for the fluid sub-problem. The same time step size of the fluid sub-problem $\Delta t_s = 0.001\text{s}$ has been used. The structure has a cylindrical cross section

with diameter $D = 0.102\text{m}$, density $\rho_s = 5.582 \times 10^3\text{kg/m}^3$, Young's modulus $E_s = 5.88 \times 10^8\text{N/m}^2$, and Poisson's ratio $\nu_s = 0.3$.

2.13.5 The Mesh Motion Problem

The coupling of the fluid and the solid problems has been realized in a strong way using a Block Gauss-Seidel coupling algorithm. The time step of the fluid problem has been imposed to be equal to the time step of the solid problem. At each time step we need to update the mesh of the fluid problem using the displacement coming from the solid computation, and on the other hand we need to transfer forces deriving from the fluid computation to the structure. This procedure is not always simple, because most of the time we have to deal with not-matching meshes, and in our case we even have different spatial dimensions for the models. The beam is in fact a mono-dimensional object, while the fluid forces are evaluated on the FSI interface, which is a 2-D surface in three-dimensional space. So the forces coming from the fluid mesh have to be properly converted into line forces. The problem is solved making the hypotheses of a non-deformable cross sections and fluid forces are obtained by circumferential integration and are transferred to the beam nodes through the shape functions of the beam. The adjoint procedure has been used to move the points of the FSI interface starting from the nodal displacement of the beam. Points of the fluid mesh which do not belong to the FSI interface are moved according to a Laplacian smoothing algorithm [8]: the equation of cell motion is solved based on the Laplacian of the diffusivity and the cell displacements. The diffusivity field is based quadratically on the inverse of the cell center distance to the FSI interface.

2.13.6 Conclusions and next steps

The so developed FSI solver will be used to gather high fidelity computational data regarding the response of a section of the cable subjected to an imposed motion matching the statistical properties of the motion in full scale. The result of such simulations will be used to feed a state-space system identification technique:

$$\mathbf{x}(k+1) = \mathbf{A}\mathbf{x}(k) + \mathbf{B}\mathbf{u}(k) \quad (18)$$

$$\mathbf{y}(k) = \mathbf{C}\mathbf{x}(k) + \mathbf{D}\mathbf{u}(k) \quad (19)$$

where $\mathbf{x}(k) \in \mathbb{R}^{n \times 1}$ is the state vector $\mathbf{y}(k) \in \mathbb{R}^{q \times 1}$ is the output vector $\mathbf{u}(k) \in \mathbb{R}^{p \times 1}$ is the input vector $\mathbf{A} \in \mathbb{R}^{n \times n}$ is the state matrix

$\mathbf{B} \in \mathbb{R}^{n \times p}$ is the input matrix $\mathbf{C} \in \mathbb{R}^{q \times p}$ is the output matrix $\mathbf{D} \in \mathbb{R}^{q \times p}$ is the feedthrough matrix. For the specific case:

- \mathbf{x} has dimension $n \times 1$ to be determined depending on the results of the system identification technique.
- $\mathbf{y} = [F_{x1}, F_{y1}, F_{x2}, F_{y2}]^T$ Is the output vector containing the transverse hydrodynamic forces at the end of the model.
- $\mathbf{u} = [x_1, y_1, x_2, y_2, \dot{x}_1, \dot{y}_1, \dot{x}_2, \dot{y}_2, \ddot{x}_1, \ddot{y}_1, \ddot{x}_2, \ddot{y}_2]^T$ is the input vector containing the transverse displacements, velocities and accelerations at the end of the model.

Only the transverse DOFs are considered because some preliminaries tests have demonstrated that the rotations may be neglected. The final aim of the work is then the development of a new finite element which can calculate the hydrodynamics forces from the instantaneous characteristics of motion. The finite element will not have additional external DOFs. Only the standard DOFs will be seen from the outside. A stiffness, damping and mass matrix due to the Hydrodynamic forces will be evaluated and the additional DOFs of the element will be only internal depending on the state vector. This new element will decrease dramatically the computational cost of the simulation and will permit to completely skip the CFD computation.

References

- [1] P. Bearman, *Circular cylinder wakes and vortex-induced vibrations*, Journal of Fluids and Structures **27** (2011), no. 5, 648–658.
- [2] R. Bourguet, G. E. Karniadakis, and M. S. Triantafyllou, *Lock-in of the vortex-induced vibrations of a long tensioned beam in shear flow*, Journal of Fluids and Structures **27** (2011), no. 5, 838–847.
- [3] J. Donea, S. Giuliani, and J. Halleux, *An arbitrary lagrangian-eulerian finite element method for transient dynamic fluid-structure interactions*, Computer methods in applied mechanics and engineering **33** (1982), no. 1, 689–723.
- [4] R. Gabbai and H. Benaroya, *An overview of modeling and experiments of vortex-induced vibration of circular cylinders*, Journal of Sound and Vibration **282** (2005), no. 3, 575–616.
- [5] H. M. Hilber, T. J. Hughes, and R. L. Taylor, *Improved numerical dissipation for time integration algorithms in structural dynamics*, Earthquake Engineering & Structural Dynamics **5** (1977), no. 3, 283–292.

- [6] K. Huang, H.-C. Chen, C.-R. Chen, et al., *Riser VIV analysis by a CFD approach*, Proceedings of the 17th International Offshore and Polar Engineering (ISOPE) Conference, Lisbon, Portugal, 2007.
- [7] A. Ibrahimbegovic, R. Niekamp, C. Kassiotis, D. Markovic, and H. G. Matthies, *Code-coupling strategy for efficient development of computer software in multiscale and multiphysics nonlinear evolution problems in computational mechanics*, Advances in Engineering Software **72** (2014), 8–17.
- [8] H. Jasak, A. Jemcov, and Z. Tukovic, *Openfoam: A c++ library for complex physics simulations*, (2013).
- [9] U. Küttler and W. A. Wall, *Fixed-point fluid–structure interaction solvers with dynamic relaxation*, Computational Mechanics **43** (2008), no. 1, 61–72.
- [10] T. Kvamsdal, J. Amundsen, and K. Okstad, *Numerical methods for fluid–structure interactions of slender structures*, Proceedings of ECCM, vol. 99, Citeseer, 1999.
- [11] H. G. Matthies, R. Niekamp, and J. Steindorf, *Algorithms for strong coupling procedures*, Computer methods in applied mechanics and engineering **195** (2006), no. 17, 2028–2049.
- [12] D. J. Newman and G. E. Karniadakis, *A direct numerical simulation study of flow past a freely vibrating cable*, Journal of Fluid Mechanics **344** (1997), 95–136.
- [13] W. Qiu, H. Lie, J. Rousset, S. Sphaier, L. Tao, X. Wang, T. Mikami, and V. Magarovskii, *Report of the Ocean Engineering Committee*, 27th International Towing Tank Conference, 2014, pp. 1–74.
- [14] P. Sagaut, *Large eddy simulations for incompressible flows*, vol. 3, Springer Berlin, 2000.
- [15] J. C. Simo and L. Vu-Quoc, *On the dynamics in space of rods undergoing large motions: a geometrically exact approach*, Computer methods in applied mechanics and engineering **66** (1988), no. 2, 125–161.
- [16] R. Taylor, *Feap. a finite element analysis program. user manual, version 8.2*, University of California at Berkeley (2008).
- [17] C. Williamson and R. Govardhan, *A brief review of recent results in vortex-induced vibrations*, Journal of Wind Engineering and Industrial Aerodynamics **96** (2008), no. 6, 713–735.

-
- [18] X. Wu, F. Ge, and Y. Hong, *A review of recent studies on vortex-induced vibrations of long slender cylinders*, Journal of Fluids and Structures **28** (2012), 292–308.
- [19] C. Yamamoto, J. Meneghini, F. Saltara, R. Fregonesi, and J. Ferrari, *Numerical simulations of vortex-induced vibration on flexible cylinders*, Journal of fluids and structures **19** (2004), no. 4, 467–489.

3 Lehre im WS 2013/2014 and SS 2014

3.1 Wintersemester 2013/2014

Advanced Object Oriented C++ Techniques	2+2	Rainer Niekamp
Weiterführendes Programmieren/ Intermediate Programming	0+4	Hermann G. Matthies, Rainer Niekamp
Einführung in das Programmieren (für Nicht-Informatiker)	0+4	Hermann G. Matthies, Rainer Niekamp
Einführung in das Wissenschaftliche Rechnen (ODE I)	2+1	Joachim Rang, Bojana Rosić
Einführung in das Parallele Rechnen	2+1	Thorsten Grahs
Visualisierung wissenschaftlicher Daten	2+1	Joachim Rang
Einführung in PDE und Numerische Methoden für PDEs	2+1	Elmar Zander, Noémi Friedman
Praktikum zum Wissenschaftlichen Rechnen	0+4	Elmar Zander
Refresher Kurse für Mathematik und Matlab	0+3	Joachim Rang und Elmar Zander

3.2 Sommersemester 2014

Fortgeschrittene Methoden für ODEs und DAEs	2+1	Joachim Rang, Bojana Rosić
Numerische Methoden für PDEs	2+1	Hermann G. Matthies, Noémi Friedman
Uncertainty Quantification, Parametric Problems, and MOR	2+1	Hermann G. Matthies, Elmar Zander
Partitioned Methods for Multifield Problems	2+1	Joachim Rang
Advanced Object Oriented C++ Techniques	2+2	Rainer Niekamp
Seminar zum wissenschaftlichen Rechnen	0+2	Hermann G. Matthies, Elmar Zander
Weiterführendes Programmieren/ Intermediate Programming	0+4	Hermann G. Matthies, Rainer Niekamp
Einführung in das Programmieren (für Nicht-Informatiker)	0+4	Hermann G. Matthies, Rainer Niekamp
Praktikum zum Wissenschaftlichen Rechnen	0+4	Hermann G. Matthies, Alexander Litvinenko
Software Entwicklungspraktikum	0+4	Hermann G. Matthies, Elmar Zander
Parallel Computing I	3+1	Thorsten Grahs

4 Veröffentlichungen und Vorträge

4.1 Schriften und Proceedings

- [1] G. Arcangioli, V. Chiarello, E. Caporali, and T. Pileggi, *Development of a webGIS for monitoring hydrological extremes in Tuscany*, Proceedings of 18th National conference of Italian Federation of the Scientific Associations for Territory and Environmental Information, Asita 2014, 2014, pp. 91–92.
- [2] E. Caporali, V. Chiarello, and G. Rossi, *Regional frequency analysis of extreme rainfall events in Tuscany*, Proceedings of XXXIV National congress of hydraulics and hydraulic engineering, Idra 2014, Zaccaria Editore, 2014, pp. 263–264, URL: <http://idra14.it/?q=content/atti-e-poster-0>.
- [3] E. Caporali, V. Chiarello, and G. Rossi, *Regional Frequency Analysis of extreme rainfall events, Research for flood risk mitigation in Tuscany region. Macro-activity B - Hydrological modeling. Activity B1-Regionalization precipitation*, Tech. report, Department of Civil and Environmental Engineering, University of Firenze, 2014, URL: http://www.sir.toscana.it/supports/download/lssp_2012.pdf.
- [4] E. Caporali, V. Chiarello, and G. Rossi, *Regional frequency analysis of extreme rainfall events, Tuscany (Italy)*, Proceedings of 2014 Fall Meeting, American Geophysical Union, 2014, URL: <https://agu.confex.com/agu/fm14/preliminaryview.cgi/Paper29190.html>.
- [5] E. Caporali, S. Manetti, V. Chiarello, and S. Fatichi, *Changes in precipitation regime in Tuscany region (Italy)*, Proceedings of European Geosciences Union General Assembly, vol. 16, Geophysical Research Abstracts, 2014, URL: <http://www.geophysical-research-abstracts.net/volumes.html>.
- [6] V. Chiarello, E. Caporali, and G. Galeati, *Investigation of the SCS-CN initial abstraction ratio using a Monte Carlo simulation for the derived flood frequency curves*, Proceedings of 2014 Fall Meeting, American Geophysical Union, 2014, URL: <https://agu.confex.com/agu/fm14/preliminaryview.cgi/Paper29251.html>.
- [7] S. Dolgov, B. N. Khoromskij, A. Litvinenko, and H. G. Matthies, *Computation of the Response Surface in the Tensor Train data format*, (2014), URL: <http://arxiv.org/abs/1406.2816>.

- [8] M. Eigel, C. J. Gittelsohn, C. Schwab, and E. Zander, *Adaptive Stochastic Galerkin FEM*, CMAME (2014), also available as SAM Report 2013-01.
- [9] M. Eigel, C. J. Gittelsohn, C. Schwab, and E. Zander, *A convergent adaptive stochastic Galerkin finite element method with quasi-optimal spatial meshes*, M2AN (accepted), also available as SAM Report 2014-01.
- [10] M. Espig, W. Hackbusch, A. Litvinenko, H. G. Matthies, and P. Wähnert, *Efficient low-rank approximation of the stochastic Galerkin matrix in tensor formats*, Computers and Mathematics with Applications **67** (2014), 818–829, doi:{10.1016/j.camwa.2012.10.008}.
- [11] N. Friedman, Gy. Farkas, and A. Ibrahimbegović, *Parametric study of the elementary segment of an antiprismatic pop-up deployable lattice column*, Ybl Journal of Built Environment **2** (2014), no. 2, 65–86, doi:10.1515/jbe-2014-0011.
- [12] N. Friedman, A. Ibrahimbegović, and H. G. Matthies, *Stochastic analysis of an exotic deployable space truss system*, Engineering for Progress, Nature and People, IABSE Symposium Madrid 2014 (A. Cutillas and M. D. G. Pulido, eds.), IABSE Report, IABSE, IABSE ETH Zurich, Zurich, Switzerland, 2014, pp. 106–107, URL: <http://www.ingentaconnect.com/content/iabse/report>, doi:10.2749/222137814814027945.
- [13] L. Giraldi, D. Liu, H. G. Matthies, and A. Nouy, *To be or not to be intrusive? The "plain vanilla" Galerkin case*, SIAM Journal of Scientific Computing **36** (2014), A2720–A2744, doi:{10.1137/130942802}.
- [14] T. Grahs and C. F. Janßen, *GPU-beschleunigte Mehrphasensimulationen für komplexe maritime Anwendungen*, Proc. NAFEMS Konferenz, Berechnung und Simulation: Anwendung, Entwicklung, Trends, Bamberg, 2014.
- [15] M. Hadigol, A. Doostan, H. G. Matthies, and R. Niekamp, *Partitioned Solution of Coupled Stochastic Problems*, Numerical Simulations of Coupled Problems in Engineering (S. R. Idelsohn, ed.), Computational Methods in Applied Sciences, vol. 33, Springer Verlag, Berlin, 2014, pp. 405–422, doi:{10.1007/978-3-319-06136-8_16}.
- [16] M. Hadigol, A. Doostan, H. G. Matthies, and R. Niekamp, *Partitioned Treatment of Uncertainty in Coupled Domain Problems: A*

- separated representation approach*, *Comp. Meth. Appl. Mech. Engrng* **274** (2014), 103–124, doi:{10.1016/Lj.cma.2014.02.004}.
- [17] A. Ibrahimbegović, R. Niekamp, C. Kassiotis, D. Marković, and H. G. Matthies, *Code-coupling strategy for efficient development of computer software in multiscale and multiphysics nonlinear evolution problems in computational mechanics*, *Advances in Engineering Software* **72** (2014), 8–17, doi:{10.1016/j.advengsoft.2013.06.014}.
- [18] C. F. Janßen and T. Grahs, *Hochleistungsrechnen auf Grafikkarten für innovative Anwendungen in der Automobilindustrie*, *NAFEMS Magazin* **32** (2014), no. 4, 86 – 96.
- [19] C. F. Janßen and T. Grahs, *Realitätsprüfung – GPU-computing in der Automobilentwicklung*, *Digital Engineering* **8** (2014), 18 – 20.
- [20] S. Manetti, V. Chiarello, and E. Caporali, *Trend analysis in precipitation regime in Tuscany*, *Proceedings of XXXIV National congress of hydraulics and hydraulic engineering, Idra 2014*, Zaccaria Editore, 2014, pp. 378–379, URL: <http://idra14.it/?q=content/atti-e-poster-0>.
- [21] E. Marino, C. Lugni, G. Stabile, and C. Borri, *Coupled dynamic simulations of offshore wind turbines using linear, weakly and fully nonlinear wave models: the limitations of the second-order wave theory*, *Proceedings of the 9th International Conference on Structural Dynamics, EURODYN 2014*, Porto, Portugal, 2014, pp. 1–8, URL: http://paginas.fe.up.pt/~eurodyn2014/CD/papers/book_of_proceedings_eurodyn2014.pdf.
- [22] E. Marino, C. Lugni, G. Stabile, C. Borri, and L. Manuel, *Coupled dynamic simulations of offshore wind turbines: influence of wave modeling on the fatigue load assessment*, *Proceedings of the XIII Conference of the Italian Association for Wind Engineering (In-Vento 2014)* (L. Carassale and M. P. Repetto, eds.), Genova, Italy, 2014, pp. 1–4.
- [23] H. G. Matthies and A. Ibrahimbegović, *Stochastic multiscale coupling of inelastic processes in solid mechanics*, *Multiscale Modelling and Uncertainty Quantification of Materials and Structures* (M. Papadarakakis and G. Stefanou, eds.), vol. 3, Springer Verlag, Berlin, 2014, pp. 135–157, doi:{10.1007/978-3-319-06331-7_9}.
- [24] R. Niekamp, A. Ibrahimbegović, and H. G. Matthies, *Formulation, solution and CTL software for coupled thermomechanics systems*, *Coupled System Mechanics* **3** (2014), 1–25, doi:{10.12989/csm.2014.3.1.001}.

- [25] J. Rang, *An analysis of the Prothero-Robinson example for constructing new DIRK and ROW methods*, Journal of Computational and Applied Mathematics **262** (2014), 105–114, doi:[10.1016/j.cam.2013.09.062](https://doi.org/10.1016/j.cam.2013.09.062).
- [26] B. V. Rosić and H. G. Matthies, *Variational theory and computations in stochastic plasticity*, Archives of Computational Methods in Engineering (2014), 1–53, doi:[10.1007/s11831-014-9116-x](https://doi.org/10.1007/s11831-014-9116-x).
- [27] I. Simonetti, L. Cappiotti, H. El Safti, and H. Oumeraci, *3D Numerical Modelling of Oscillating Water Column Wave Energy Conversion Devices: Current Knowledge and OpenFOAM implementation*, 1st International Conference on Renewable Energies Offshore, RE-NEW2014, 2014, pp. 1–10.
- [28] T. Srisupattarawanit, R. Niekamp, and H. G. Matthies, *A coupled multi-physics model for dynamics of offshore wind energy converter*, Development and Applications of Oceanic Engineering (DAOE) **3**, issue **1** (2014), URL: <http://www.daoe-journal.org/paperInfo.aspx?ID=9009>.

4.2 Berichte

- [1] W. Krosche, Martin und Heinze, *A robustness analysis of a preliminary design of a cestol aircraft*, Informatik-Bericht 2014-02, TU Braunschweig, Braunschweig, 2014, URL: <http://www.digibib.tu-bs.de/?docid=00055746>.
- [2] J. Rang, *An analysis of the Prothero–Robinson example for constructing new adaptive ESDIRK methods of order 3 and 4*, Informatik-Bericht 2014-06, TU Braunschweig, Braunschweig, 2014, URL: <http://www.digibib.tu-bs.de/?docid=00056090>.
- [3] J. Rang, *Adaptive timestep control for fully implicit Runge–Kutta methods of higher order*, Informatik-Bericht 2014-03, TU Braunschweig, Braunschweig, 2014, URL: <http://www.digibib.tu-bs.de/?docid=00055783>.
- [4] J. Rang, *The Prothero and Robinson example: Convergence studies for Runge–Kutta and Rosenbrock–Wanner methods*, Informatik-Bericht 2014-08, TU Braunschweig, Braunschweig, 2014, URL: <http://www.digibib.tu-bs.de/?docid=00057194>.
- [5] J. Rang and R. Niekamp, *A component framework for the parallel solution of the incompressible Navier-Stokes equations*

with *Radau-IIA methods*, Informatik-Bericht 2014-07, TU Braunschweig, Braunschweig, 2014, URL: <http://www.digibib.tu-bs.de/?docid=00056708>.

- [6] B. Rosić and J. Diekmann, *Methods for the uncertainty quantification of aircraft simulation models*, Informatik-Bericht 2014-01, TU Braunschweig, Braunschweig, 2014, URL: <http://www.digibib.tu-bs.de/?docid=00055749>.
- [7] J. Waeytens and Rosić, *Comparison of deterministic and probabilistic approaches to identify the dynamic moving load and damages of a reinforced concrete beam*, Informatik-Bericht 2014-09, TU Braunschweig, Braunschweig, 2014, URL: <http://www.digibib.tu-bs.de/?docid=00057886>.

4.3 Vorträge

Giacomo Arcangioli, Valentina Chiarello and Enrica Caporali and Tiziana Pileggi, *Development of a webGIS for monitoring hydrological extremes in Tuscany*, ASITA2014, Firenze, Italy, 14.-16.10.2014

Enrica Caporali, Simona Manetti, Valentina Chiarello and Simone Fatichi, *Changes in precipitation regime in Tuscany Region (Italy)*, EGU General Assembly 2014, Vienna, Austria, 27.04-02.05.2014

Enrica Caporali, Valentina Chiarello and Giuseppe Rossi, *Regional Frequency Analysis of extreme rainfall events in Tuscany*, IDRA2014, Bari, Italy, 07.-10.09.2014

Noémi Friedman, Adnan Ibrahimbegović, and Hermann G. Matthies *Stochastic Analysis of an Exotic Deployable Space Truss System*, IABSE 2014, Madrid, Spain, 3-5. September 2014

Noémi Friedman, Adnan Ibrahimbegović, and Hermann G. Matthies *Uncertainties in the Deployment of a Highly Flexible Space Truss System*, ISCM-36 Israel Symposium, Haifa, Israel, 24. April 2014

Simona Manetti, Valentina Chiarello and Enrica Caporali, *Trend analysis in precipitation regime in Tuscany*, IDRA2014, Bari, Italy, 07.-10.09.2014

Hermann G. Matthies, *A stochastic setting and tensor methods for inverse problems*, Sandia Laboratories, Livermore, CA, USA, 8.1.14

Hermann G. Matthies, *Uncertainty quantification and inverse problems*, Berkley University, CA, USA, 9.1.14

- Hermann G. Matthies, *Parametric and inverse problems with uncertainty quantification and Parameter identification and tensor approximation*, Boulder University, CO, USA, 14. and 17.1.14
- Hermann G. Matthies, *Parametric problems, uncertainty quantification and inverse problems* and em Tensor approximations for inverse problems, MIT, Cambridge, MASS, USA 22. and 23.1.14
- Hermann G. Matthies, *Representations of heterogeneous material properties*, The University of Newcastle, Callaghan, NSW, Australia, 6.2.14
- Hermann G. Matthies, *Non-intrusive uncertainty quantification and inverse problems*, Swansea University, UK, 27.-29.5.14
- Hermann G. Matthies, *Factorisations, Tensor Methods, and Inverse Problems* TU Berlin, 10.-11.6.14
- Hermann G. Matthies, *Uncertainty, Quantification, Risk and Reliability, Extreme Events*, Dt.-Ital. Graduiertenkolleg, TU Braunschweig, 8.7.2014
- Hermann G. Matthies, *Coupled Stochastic Problems* WCCM, Barcelona, Spain, 21.-24.7.14
- Hermann G. Matthies, *Stochastic Models, Uncertainty Quantification, and Inverse Problems with Low-Rank Tensor Approximations* Cambridge, UK, 8.-31.7.14
- Hermann G. Matthies, *Inverse Problems and Identification by Bayesian Methods* Summer School on Modeling and Numerical Methods for Uncertainty Quantification, Porquerolles, France, 1.-6.9.14
- Hermann G. Matthies, Keynote Lecture *Non-intrusive stochastic Galerkin methods and inverse problems*, NASPDE, Lausanne, Switzerland, 9.-11.9.14
- Hermann G. Matthies, *To be or not to be Intrusive? Solution of stochastic and parametric equations* TU Berlin, 17.12.14
- Hermann G. Matthies et al., *Non-linear Bayesian updates and low-rank approximations*, SIAM Conference on Uncertainty Quantification USA, Savannah, Georgia, 31.3.-3.4.14
- Joachim Rang, *Time-adaptive methods for the incompressible Navier-Stokes equations with high order accuracy in the pressure component*, Vortrag im Institutskolloquium Mathematik und Naturwissenschaften, Universität Kassel, Mai 2014.

Joachim Rang, *Solution of stiff ODEs and DAEs with Runge-Kutta and Rosenbrock-Wanner methods*, Vortrag im C²A²S²E² Brown Bag Seminar, DLR, Braunschweig, Juli 2014.

Joachim Rang, *A class of parallel time-adaptive methods for the incompressible Navier-Stokes equations with high order accuracy in the pressure component*, FEM Symposium Chemnitz, TU Chemnitz, Germany, September 2014.

Giovanni Stabile, *FSI with OpenFOAM using the Component Template Library (CTL)*, NoFUN meeting 2014, TU Braunschweig, Germany, 24 September 2014

Bojana Rosić, Jan Sýkorá, Anna Kučerová and Hermann G. Matthies, *A Bayesian approach to linear and nonlinear identification problems*, ESCO 2014. 4th European Seminar on Computing, Pilsen, Czech Republic, June 15-20, 2014

Julien Wayetens and Bojana Rosić, *Comparison of deterministic and probabilistic approaches to identify the dynamic moving load of a reinforced concrete beam*, ESCO 2014. 4th European Seminar on Computing Pilsen, Czech Republic, June 15-20, 2014

Bojana Rosić, *A Bayesian Approach to Linear and Nonlinear Identification Problems*, GAMM Annual Meeting, Erlangen, 10.-14.03.2014

Bojana Rosić and Hermann G. Matthies, *Identification of elastoplastic material properties in a Bayesian setting*, WCCM 2014, Barcelona, Spain, 20.-25.07.2014

Muhammad Sadiq Sarfaraz and Hermann G. Matthies, *Stochastic non-local material models of irreversible behaviour*, IRTG 1627, Evaluation Presentation, Institut für Kontinuumsmechanik der LU Hannover, 3.12.2014

Muhammad Sadiq Sarfaraz and Hermann G. Matthies, *Stochastic non-local material models of irreversible behaviour*, Poster session in DFG Evaluation program, Institut für Kontinuumsmechanik der LU Hannover, 9.0.2014

4.4 Projekttreffen

Noémi Friedman, Joachim Rang, *Quantifizierung von Unsicherheiten*, SFB 880 Quartalstreffen im Projektbereich C

Hermann G. Matthies, Kick-off Meeting for SPP 1748 Reliable simulation techniques in solid mechanics. Development of non-standard

discretization methods, mechanical and mathematical analysis. Essen, 28.10.2014

Hermann G. Matthies, 25th Plenary Meeting im German-Italian Doctoral Exchange Programme, Braunschweig, 5.-7.5.2014

Hermann G. Matthies, 26th Plenary Meeting im German-Italian Doctoral Exchange Programme, Florence, Italy, 6.-8.11.2014

Hermann G. Matthies, M. Sadiq Sarfaraz, Projekttreffen of the IRTG 1627 in Hannover, 5.6.14

Noémi Friedman, Bojana Rosić, Joachim Rang, Hermann G. Matthies *Uncertainty Quantification - Newly Implemented Features in the Stochastic Software*, SFB880-Quartalstreffen Bereich C - 2014/1, 08.01.2014

Noémi Friedman, Bojana Rosić, Joachim Rang, Hermann G. Matthies *Uncertainty Quantification - Non-intrusive Galerkin Method*, SFB880-Quartalstreffen Bereich C - 2014/2, 06.05.2014

Noémi Friedman, Bojana Rosić, Joachim Rang, Hermann G. Matthies *Uncertainty Quantification of the Dynamic Simulation Model of the High Lift Aircraft*, SFB880-Quartalstreffen Bereich C - 2014/3, 18.09.2014

Noémi Friedman, Joachim Rang, Hermann G. Matthies *Summary of UQ*, SFB880-Quartalstreffen Bereich C - 2014/4, 02.12.2014

Noémi Friedman, Bojana Rosić, Joachim Rang, Hermann G. Matthies *Analysis of the propagation of uncertainties in the dynamic simulation model of the aircraft*, SFB880-Forschungsklausur - 2014, Braunlage, 13-14.10.2014

Noémi Friedman, Joachim Rang, *Quantifizierung von Unsicherheiten*, SFB 880 Forschungsklausur, Braunlage, 13.-14.09.2014

4.5 Organisation von Minisymposia/Konferenzen

Martin Eigel, Loïc Girardi, Alexander Litvinenko, Hermann Matthies, and Anthony Nouy, Minisymposium *Low-rank and sparse representation methods for uncertainty quantification*, SIAM Conference on Uncertainty Quantification USA, Savannah, Georgia, March 31-April 03, 2014.

Bojana Rosić, GAMM Junior Workshop at TU Braunschweig, Institute of Scientific Computing, 9.-10.10.14

Bojana Rosić, Minisymposium *Parameter Identification in a probabilistic setting* ESCO 2014. 4th European Seminar on Computing, Pilsen, Czech Republic, June 15-20, 2014

4.6 Teilnahme und Lehre an Workshops und Weiterbildung

Thorsten Grahs, OpenFOAM introduction, March, September and December 2014, TU Braunschweig

Thorsten Grahs, OpenFOAM advanced, March and September 2014, TU Braunschweig

Thorsten Grahs, OpenFOAM programming, September 2014, TU Braunschweig

Thorsten Grahs, OpenFOAM Thermo simulation, December 2014, TU Braunschweig

Thorsten Grahs, **2nd Northern Germany OpenFoam User Meeting** NOFUN 2014, Braunschweig, Haus d. Wissenschaften, 24.09.2014.

With participants from DLR, FH Kiel, TU Berlin, Univ. Rostock, LU Hannover, TU Braunschweig, BETA systems, CPU 24|7, Engys

4.7 Habilitation und Dissertationen

Alberto Ciavattone, *Seismic vulnerability analysis for masonry hospital structures: expeditious and detailed methods*, 6.5.14

4.8 Abschluss- und Studienarbeiten

Ning Chen *Gaps Interpolation of Meteorological Data using Neural Networks and Geostatistical Methods*, Masterarbeit. Supervisor: Joachim Rang

Denes Glavaticy, *Tensegrity az epitoiparban (Tensegrity structures in civil engineering)*, Dpt. of Structural Eng., Budapest, Hungary, Fac. of Civil Eng., Univ. of Technology and Economics, Co-supervisor: Noémi Friedman

5 Sonstiges

5.1 Gäste am Institut

Dr. Milos Ivanović, Assistant Professor at the Department of Mathematics and Informatics, University of Kragujevac, Kragujevac, Ser-

bia, *Dealing with Parameter Estimation and State Update in Hydrological Modeling*, 27.-31.1.14

Mijo Nikolić, co-tutelle Ph.D. student at the École Normale Supérieure de Cachan, LMT, Civil/Structural/Materials Engineering, Cachan, France, and University of Split, Faculty of Civil Engineering, Architecture and Geodesy, 4.2.-1.5.14

Prof. Dr. KC Park em., Department of Aerospace Engineering Sciences, University of Colorado, Boulder, CO, USA, *A Simultaneous Tailoring of Flexible Structures and Feedback Control: an Interdisciplinary Approach*, 15-19.7.14

Prof. Dr. Roger Ohayon, Conservatoire National des Arts et Métiers (CNAM) Paris, 12.-16.5.14, 22.-28.5.14

Dr. Matteo Capaldo, École Normale Supérieure de Cachan, LMT (ENS Cachan/CNRS/UPMC/PRES), Cachan, France, *An approximation framework for PGD-based non-linear solver*, 17.-21.11.14

Dr. Abhishek Kundu, College of Engineering, Swansea University, Swansea, UK, *Framework for total Uncertainty Quantification in Computational Mechanics*, 24.-28.11.14

Masumeh Mohammadi, Ph.D. student at Universität Würzburg, Lehrstuhl für Mathematik IX, *Analysis of discretization schemes for Fokker-Planck equations and related optimality systems*, 2.12.14

5.2 Einladungen an Mitglieder des Instituts

5.3 Board Memberships

Professor Matthies is Associate Editor for the *ASA- and SIAM Journal on Uncertainty Quantification* as well as a member of the Editorial Advisory Board for the recently launched journal *Advanced Modelling and Simulation in Engineering Sciences* (AMSES).

He is also a member of the Advisory Boards of the SRI - Center for Uncertainty Quantification in Computational Science Engineering at King Abdulla University of Science and Technology (KAUST), Saudi Arabia, and of the Editorial Board of *Coupled Systems Mechanics* (CSM).

5.4 Beteiligung am IRTG 1627

On 27th May, 2010, the Senate for Research Training Groups of the DFG (Deutsche Forschungsgemeinschaft) decided to fund the proposal

of Leibniz Universität Hannover for the International Research Training Group on „Virtual Materials and Structures and their Validation“.

The training group, which is incorporated in the Graduate School MUSIC at Leibniz Universität Hannover, started its work in October 2010. From our institute, Mohammad Sadiq Sarfaraz joined the group in April 2014 to work on his PhD. Besides him PhD students and principal investigators from Leibniz Universität Hannover as well as from École Normale Supérieure Cachan, France are involved. The aim of the International Research Training Group is to set up a forum for research and development of newest methods related to computational technologies, virtual testing and validation. The emphasis is to provide a place in which gifted Master students, PhD Students and Post-docs can perform leading international research in the interdisciplinary area of the application of virtual testing methods to materials and structures. Due to the participation of scientists and teachers from different fields such as Mechanics and Computational Mechanics, Civil and Mechanical Engineering and Applied Mathematics, the knowledge base is broadened. New insights are gained by the interdisciplinary cooperation. Thus, the Research Training Group provides a stimulating education and research environment for young scientists. Strong interaction with leading scientists from France in the area of multi-scale techniques, experimental methods and composite structures complete the scientific approaches and the educational spectrum.

5.5 Beteiligung am Projekt „Isogeometric and stochastic collocation methods for nonlinear, probabilistic multi-scale problems in continuum mechanics“ im SPP 1748

In this project, we intend to use the newly developed concept of isogeometric collocation (IGA-C) in combination with stochastic collocation (SC) to achieve stable and computationally efficient higher-order modeling of irreversible multiscale behaviour in solid mechanics. The basic assumption is that the microstructure of a heterogeneous solid is uncertain and hence should be modeled probabilistically. In order to describe the effects of the microscale uncertainty not only on the mean macroscopic fields, but also on their variability, a probabilistic treatment of the scale transition, is also needed. As the computational cost of such stochastic computations may be orders of magnitude higher than that of simple deterministic analyses, an unprecedented computational efficiency is sought in the combination of IGA-C for the mechanical/deterministic modeling, and of an SC scheme with novel ansatz functions for the stochastic discretization. The numerical framework to be developed encompasses local and nonlocal elasticity and plasticity with finite

strains, as well as contact, damage and fracture models.

This research is carried out within the framework of the DFG-Schwerpunktprogramms SPP 1748 „Reliable Simulation Techniques in Solid Mechanics. Development of Non-standard Discretisation Methods, Mechanical and Mathematical Analysis.“ For more information on the SPP 1748 please refer to <http://gepris.dfg.de/gepris/projekt/237201391>.

5.6 Beteiligung am SFB 880 Fundamentals of High Lift for Future Civil Aircraft

The second phase of this project was granted in December 2014.

The Coordinated Research Centre 880 develops the fundamentals of active high-lift for environmentally friendly future transport aircraft. The research is motivated by growing demands for air travel in economic zones like Europe. Sustainable growth can only be achieved here by using new means of transport, which enable efficient point-to-point connections, short runways for take-off and landing, drastic reductions of aircraft noise, and low fuel consumption. This requires fundamental research in aeroacoustics, in methodology for efficient active high-lift, and in flight dynamics.

Our project does research on the „Uncertainties quantification in models for high-lift simulations“. It quantifies and identifies the uncertainties in selected simulations of the Collaboratory Research Centre. In the first funding period, the flight mechanical model and the aircraft design method were considered. The developed methods for stochastic forward problems need further improvements such that they can be used for identification in the area of Bayes inverse analysis. Further applications include the identification of parameters in the turbulence models of flows along porous media, and the stochastic characterization of experimental scans of these media. An international research training group is integrated into the SFB 880.

For more information on the SFB 880 please refer to <https://www.tu-braunschweig.de/sfb880>.

5.7 Beteiligung am Studiengang CSE

Professor Matthies ist stellvertretender Sprecher des internationalen Master-Studiengangs Computational Sciences in Engineering (CSE).

Technische Universität Braunschweig was the first German university to offer this international study course.

Computer simulation has strongly gained in importance for engineering and natural sciences and has become an indispensable part of almost all scientific research and technological development at universities as well as in research and development offices in the private sector.

The breathtaking progress in computing has dramatically changed the way engineers, mathematicians, and computer scientists work. In many areas computer simulations have complemented or even replaced experiments, which has led to a previously unknown quality of scientific and practical work. The technological improvement of hard- and software and the development of computer-based methods have opened up new possibilities for the natural sciences and engineering.

People with networking skills who are able to connect knowledge of engineering, applied mathematics and computer sciences are in demand.

Possible directions of study are Civil Engineering, Mechanical Engineering, Electrical Engineering, and Mathematics and Computer Science.

Due to the international focus of the CSE study programme, our students find themselves in a multicultural environment, and foreign guest lecturers add to our curriculum on a regular basis. CSE students get the opportunity to take advantage of our international cooperations with renowned research institutions in France, Great Britain and Spain (travel grants are available).

The Master of Science (M.Sc.) degree in the international, interdisciplinary and bilingual programme CSE opens up a wide range of professional prospects on a globalised job market. Graduated students are qualified for a scientific career and leading positions in research and development of international high-tech industry such as the automotive, aeronautical, chemical and software engineering industries.

For more information on the CSE study programme please refer to <http://www.tu-braunschweig.de/cse>.